AGU PUBLICATIONS

JGR

Journal of Geophysical Research: Atmospheres

RESEARCH ARTICLE
10.1002/2015JD024153

Key Points:
- Simultaneous measurements of the hygroscopicity for BC-containing and BC-free particles using an SP2
- Laboratory experiments using internally mixed particles of BC and ammonium sulfate
- Similar hygroscopicity parameter for BC-coating materials and BC-free particles in urban air

Correspondence to:
S. Ohata,
ohata@eps.s.u-tokyo.ac.jp

Citation:
Ohata, S., J. P. Schwarz, N. Moteki, M. Koike, A. Takami, and Y. Kondo (2016), Hygroscopicity of materials internally mixed with black carbon measured in Tokyo, *J. Geophys. Res. Atmos.*, *121*, 362–381, doi:10.1002/2015JD024153.

Received 29 AUG 2015
Accepted 10 DEC 2015
Accepted article online 15 DEC 2015
Published online 14 JAN 2016

Hygroscopicity of materials internally mixed with black carbon measured in Tokyo

Sho Ohata[1], Joshua P. Schwarz[2], Nobuhiro Moteki[1], Makoto Koike[1], Akinori Takami[3], and Yutaka Kondo[4]

[1]Department of Earth and Planetary Science, Graduate School of Science, University of Tokyo, Tokyo, Japan, [2]Chemical Sciences Division, Earth System Research Laboratory, National Oceanic and Atmospheric Administration, Boulder, Colorado, USA, [3]Regional Atmospheric Environment Section, Center for Regional Environmental Research, National Institute for Environmental Studies, Tsukuba, Japan, [4]National Institute of Polar Research, Tokyo, Japan

Abstract Black carbon (BC) aerosols become internally mixed with non-BC compounds (BC coatings) during aging in the atmosphere. In this study, we measured the hygroscopicity parameter κ on a single-particle basis for both BC-coating materials ($\kappa_{\text{BC-coat}}$) and BC-free particles ($\kappa_{\text{BC-free}}$) in the urban atmosphere of Tokyo, using a single-particle soot photometer (SP2). In our measurement system, dry ambient particles were first mass selected by an aerosol particle mass analyzer, then humidified, and then passed to the SP2 for detection of their refractory BC mass content and optical diameter. A quadrupole aerosol mass spectrometer was also employed to interpret the hygroscopicity data. During the observation period, the measured $\kappa_{\text{BC-coat}}$ generally agreed with $\kappa_{\text{BC-free}}$ to within ±25% and was usually in typical range for inorganic and organic aerosols. These results indicate that BC-coating materials and BC-free particles in Tokyo usually had similar chemical compositions, internal mixtures of inorganic and organic compounds, even in a source region. However, occasionally $\kappa_{\text{BC-coat}}$ was much higher than $\kappa_{\text{BC-free}}$ values, when the mass concentrations of BC and organic aerosols were poorly correlated. This indicates external mixing of BC-containing and BC-free particles from different sources. These findings improve our understanding of the cloud condensation nuclei activity of BC-containing particles, which strongly influences their wet removal, and optical properties in the ambient air.

1. Introduction

Black carbon (BC) aerosols are emitted by incomplete combustion of carbonaceous matter such as fossil fuels and biomass. They absorb solar radiation and contribute to positive radiative forcing [*Bond et al.*, 2013; *Intergovernmental Panel on Climate Change*, 2013; *Kondo*, 2015]. BC aerosols are become increasingly internally mixed with non-BC (inorganic, organic, or inorganic + organic) compounds during aging after their initial emission [*Schneider et al.*, 2005; *Shiraiwa et al.*, 2007; *Matsui et al.*, 2013]. Because BC itself is generally not water active, the hygroscopic growth of BC-containing particles strongly depends on the amount and chemical composition of the materials internally mixed with BC in individual particles [*McMeeking et al.*, 2011; *Liu et al.*, 2013]. Improved understanding of the hygroscopicity of BC-coating materials is important because it can largely influence both the cloud condensation nuclei properties (or the wet removal) and the optical properties of BC-containing particles in the atmosphere [e.g., *Zhang et al.*, 2008; *Oshima et al.*, 2009].

To directly measure the hygroscopicity of BC-coating materials, one approach is to combine single-particle-based detection of BC-containing particles with techniques for measuring the hygroscopicity of bulk aerosol. A single-particle soot photometer (SP2, Droplet Measurement Technology, Boulder, CO, USA), which utilizes a laser-induced incandescence technique, can optically distinguish individual BC-free and BC-containing particles [*Stephens et al.*, 2003; *Schwarz et al.*, 2006; *Moteki and Kondo*, 2007, 2010]. *McMeeking et al.* [2011] combined the SP2 with the hygroscopic tandem differential mobility analyzer (HTDMA) [e.g., *Duplissy et al.*, 2009] to quantify the mobility hygroscopic growth of BC-containing particles. *Liu et al.* [2013] applied the HTDMA-SP2 system to field observations of aerosols and showed the importance of the effect of BC mixing state on the hygroscopic properties of BC-containing particles. *Schwarz et al.* [2015] developed a humidified SP2 (h-SP2) by modifying the standard (dry) SP2 and thereby quantified the BC mass content and optical diameter of individual aerosol particles under a controlled relative humidity (RH). They combined the h-SP2 with a standard (dry) SP2 to quantify the hygroscopic growth of BC-containing particles and applied the measurement system in aircraft observations. However, relatively few measurement data of the hygroscopic properties of ambient BC-containing particles currently exist. Of particular use are simultaneous measurement data of the hygropicity parameter κ

[*Petters and Kreidenweis*, 2007] for ambient BC-free particles ($\kappa_{BC\text{-}free}$) and BC-coating materials ($\kappa_{BC\text{-}coat}$). The difference between $\kappa_{BC\text{-}free}$ and $\kappa_{BC\text{-}coat}$ reflects the difference of chemical compositions between BC-free particles and BC-coating materials. Therefore, simultaneous measurements of $\kappa_{BC\text{-}free}$ and $\kappa_{BC\text{-}coat}$ can provide information on mixing states of BC and non-BC aerosols. This kind of measurement enables evaluations of the validity of representing the chemical composition of BC-coating materials as that of aerosols measured by a bulk chemical analysis, a commonly made assumption [*Moteki et al*., 2007; *Shiraiwa et al*., 2007, 2008]. Furthermore, in numerical model calculations, it is generally assumed that condensable materials are partitioned to BC and BC-free particles in concurrent condensation processes [e.g., *Matsui et al*., 2013], another assumption that can be tested via comparison of $\kappa_{BC\text{-}free}$ and $\kappa_{BC\text{-}coat}$.

In this study, we characterized the hygroscopic growth of BC-free and BC-containing particles in the urban atmosphere of Tokyo. To measure the hygroscopic growth factor (GF) of individual BC-free and BC-containing particles with a specific dry particle mass, we humidified an SP2 (to an h-SP2) and deployed it in conjunction with an aerosol particle mass analyzer (APM, Model 3601, KANOMAX, Osaka, Japan). Thus, we measured $\kappa_{BC\text{-}free}$ and $\kappa_{BC\text{-}coat}$ simultaneously.

In this paper, the characteristics of the standard and humidified SP2s are described first, followed by the descriptions of the configuration of the measurement system and the data-processing procedure. We tested the approach in the laboratory with well-characterized BC-free and BC-containing particles and then applied the method to ambient aerosol observations in Tokyo.

Note that throughout this study, "black carbon" is identified by the SP2 with a laser-induced incandescence technique and therefore corresponds to "refractory black carbon (rBC)" in the terminology recommended by *Petzold et al*. [2013]. Particles that contain both BC and non-BC materials are termed BC-containing particles. For convenience, BC and the non-BC fraction within a BC-containing particle are sometimes called the BC core and the BC coating, respectively; here we do not intend to suggest knowledge of actual particle morphology with the use of these terms. Furthermore, BC particles with little-enough coating materials (i.e., less than the SP2 detection limit) are sometimes referred to as bare BC particles.

2. Methods

2.1. Single-Particle Soot Photometer

The standard SP2 measures both the BC mass content and the optical diameter of individual aerosol particles under dry conditions (<20% RH) by detecting both the laser-induced incandescence emitted from and the laser light scattered by each particle. Because the details of the SP2 can be seen elsewhere [*Stephens et al*., 2003; *Schwarz et al*., 2006; *Moteki and Kondo*, 2007, 2010], the characteristics of the SP2 are only briefly described here. In the SP2, sample air containing aerosol particles is introduced into a Nd:YAG laser beam ($\lambda = 1064$ nm). During transit in the laser beam, a BC-free particle (a nonlight-absorbing particle) elastically scatters laser light. The intensity of the light scattered from each BC-free particle is detected by an avalanche photodiode detector (APD), and the optical diameters of the particles are determined by assuming their refractive indices and spherical shape. The BC core within a BC-containing particle, on the other hand, absorbs enough energy from the laser to heat up to its vaporization temperature (about 4200 K) and at that temperature emits visible thermal light (incandescence). The intensity of the incandescence emitted from each BC core is measured with photomultiplier tubes and is uniquely related to the mass of the BC core ($m_{BC\text{-}core}$). The mass-equivalent diameter of the BC core ($D_{BC\text{-}core}$) is determined by assuming that the true (void-free) density of the BC component ($\rho_{BC\text{-}core}$) is 1.8 g cm^{-3}, as discussed in *Moteki et al*. [2010]. The size range of $D_{BC\text{-}core}$ detected by the SP2 is between 70 and 850 nm. The detection range of optical diameters of BC-free particles is between 170 and 850 nm. Note that throughout this paper the term "BC-free particles" is used for particles that do not emit thermal light detectable by SP2, and therefore, it is possible that aerosol particles that contain BC cores with diameters smaller than about 50 nm are counted as BC-free particles, if optical diameters are in the SP2 detection range. Some fractions of particles containing BC cores with diameters between 50 and 70 nm are detected but excluded in the data analysis.

In addition, the SP2 quantifies the dry diameter of BC-containing particles ($D_{BC\text{-}shell}$). Just at the edge of the laser beam, evaporation of the non-BC component can be ignored. Therefore, detection of the scattered light at the edge of the Gaussian laser beam by the APD and a position-sensitive APD enables measurement of the

differential scattering cross section of the whole, dry, unperturbed BC-containing particle integrated over the solid angle of SP2 detectors [*Gao et al*., 2007]. Thus, the $D_{\text{BC-shell}}$ can be quantified, assuming refractive indices of BC and non-BC components and a core-shell structure for BC-containing particles.

As indicators of the relative coating amount of individual BC-containing particles, we define dry shell/core diameter ratio (R_{D}) and dry (shell + core)/core mass ratio (R_{m}) as

$$R_D = \frac{D_{\text{BC -shell}}}{D_{\text{BC-core}}}, \tag{1}$$

and

$$R_m = \frac{m_{\text{d}}}{m_{\text{BC-core}}} = 1 + \frac{\rho_{\text{non-BC}}}{\rho_{\text{BC-core}}}\left(R_D^3 - 1\right), \tag{2}$$

respectively, where m_{d} is dry particle mass of the BC-containing particle and $\rho_{\text{non-BC}}$ is void-free density of BC-coating materials. The R_{D} can be determined by measuring $D_{\text{BC-core}}$ and $D_{\text{BC-shell}}$, as described above (SP2-scattering method). Under the assumption of the densities, the R_{m} can be derived from R_{D} by equation (2). In addition to the SP2-scattering method, dry BC-coating amount can be also quantified by an APM-SP2 measurement system, where the APM first selects dry particles with specific m_{d} and then the SP2 measures $m_{\text{BC-core}}$ of individual particles (APM method; a schematic diagram shown in Figure A1). In the APM method, the R_{m} ($= m_{\text{d}}/m_{\text{BC-core}}$) is the measured variable, and R_{D} can be derived from R_{m} by equation (2), assuming $\rho_{\text{BC-core}}$, $\rho_{\text{non-BC}}$, and core-shell geometry. These two methods are evaluated using laboratory-generated BC-containing particles in section A1. To the best of the author's knowledge, this is the first application of the APM-SP2 system for quantifying BC-coating mass, although the system has been employed for calibrating SP2 in previous studies [e.g., *Moteki and Kondo*, 2010; *Laborde et al*., 2012]. This technique is further applied to the measurements of hygroscopicity of individual particles, as detailed in section 2.3. In this study, we define "thinly coated BC particles" and "thickly coated BC particles" as particles that have coatings of $R_{\text{m}} = 1.2$–1.8 and $R_{\text{m}} = 6.4$–9.7, respectively.

2.2. Humidified-SP2

We modified the SP2 (h-SP2) to quantify the BC mass content and optical diameter of individual aerosol particles under a controlled RH. The technical details of the method to control RH in the h-SP2 are seen in *Schwarz et al*. [2015]. Here we describe the systems for flow control of the h-SP2 used specifically for this study.

In the detector chamber of the SP2, particle-free sheath air cylindrically surrounds the sample (aerosol-containing) air to constrain the aerosol particles to the center one fourth of the laser beam with high stability. To measure the optical size of the BC-containing particles under the specific RH condition, the RH of both the sample air and the sheath air must be controlled. Figure 1 shows a schematic of the flow system of the h-SP2 used in this study. The sample air and sheath air are independently humidified by separate humidification units, which each consist of two Nafion water-permeable tubes (TT-110; Perma Pure LLC, Toms River, NJ, USA), an aluminum water bath, and Peltier elements with fans, as detailed in *Schwarz et al*. [2015]. After humidification, the sample air passes through a one-fourth-inch stainless steel (SS) tube with a length of about 180 cm with several bends, in order to achieve equilibrium between aerosol particles and water vapor. The sample air is then split into the sample flow and a bypass flow. The sample flow is introduced into the detector chamber for particle measurement, whereas the bypass flow is introduced into an RH/temperature probe assembly (Vaisala HMP60; Helsinki, Finland). By using the bypass flow for measurement of the RH of the sample air, particle loss in the assembly is minimized in our setup. The sheath flow is particle free, and the RH of the sheath air is monitored by another RH/temperature probe assembly just before the sheath air enters the detector chamber. The detector chamber, RH measurement units, and SS tube for equilibrium are contained within a thermally isolated volume within an insulating blanket, thereby minimizing fluctuations of the temperature and RH of the sample air and sheath air after passing through the humidification units. As this work was conducted in laboratory conditions, temperature gradients and fluctuations were minimal.

The residence time of the sample air in the SS tube depends on the sample and bypass flow rates. In this study, the sample, bypass, and sheath flow rates were set at 2.0, 4.7, and 16.7 $\text{cm}^3\,\text{s}^{-1}$ at a room temperature (~298 K) and pressure (~1013 hPa), respectively. Under these operating conditions, the residence time is

estimated to be 3.4 s, which is generally sufficient for aerosol particles to achieve equilibrium before sizing in the detector chamber. *Chuang* [2003] conducted a field study of the hygroscopic growth of aerosol particles in Mexico City and reported that a limited number fraction (0–2.0%) of aerosol particles required a residence time of longer than 2–3 s to reach equilibrium hygroscopic growth at ~90% RH. *Sjogren et al*. [2007] confirmed that equilibration of pure ammonium sulfate (AS) is fast (<1 s) and showed that even for aerosol particles that required longer than 40 s to reach equilibrium at 85% RH, a 4 s residence time was sufficient to measure equilibrium GF with an uncertainty of 7%. Using a simple model of the time-dependent water uptake by aerosol, *Schwarz et al*. [2015] found that the measured $\kappa_{\text{BC-coat}}$ at 90% RH at a residence time of 4.9 s for BC-containing particles with $D_{\text{BC-core}} = 175$ nm, $R_{\text{D}} = 2.14$, and $\kappa_{\text{BC-coat}} = 0.5$ can be underestimated by 35%. However, this underestimate quickly becomes negligible at lower RH, for smaller volume particles, and for particles with lower $\kappa_{\text{BC-coat}}$. Therefore, although the hygroscopic growth of some particles can be underestimated because of their slow water uptake, the measurement uncertainty due to this effect should not be statistically significant in the current h-SP2 system and was not evaluated further in this study.

During a field campaign in Tokyo in July–August 2014 (section 3), the RH of the sample and sheath air were 85% with precision 0.3%. The RH/temperature probes were calibrated using a chilled mirror dew point hygrometer with the absolute accuracy of ±2% (DPH-203B, Tokyo Opto-Electronics Co., Ltd., Tokyo, Japan).

2.3. APM-h-SP2 Method

2.3.1. Experimental Setup

Combining the h-SP2 with an APM allows measurement of the hygroscopic growth of individual BC-free and BC-containing particles with known dry mass. A schematic diagram of the APM-h-SP2 method is shown in Figure 2. The sample air containing the aerosol particles is dried (<10% RH) by diffusion dryers filled with silica gel and molecular sieve desiccant. The estimated residence time at dryers was 18.5 s for laboratory experiments (section 2.3.3) and 12.3 s for ambient measurements, where the dry flow was shared with the other instruments (section 3). The estimated residence time after drying and before mass selection was 5.9 s and 2.0 s for laboratory and ambient measurements, respectively. Particles of a given dry mass-to-charge ratio (at mass m_{d}) are selected by the APM prior to h-SP2 measurements. The width of the transfer function of the APM under the operating conditions was theoretically estimated to be less than about ±16% of the selected particle mass [*Tajima et al*., 2013]. The optical diameter (D) of the selected particles under the controlled RH condition is then measured by the h-SP2, using the data-processing algorithm described in the next section. Multiply charged particles that passed through the APM were excluded in the data analysis.

The mass-equivalent dry diameter (D_{d}) of the BC-free particles is determined from m_{d}, assuming their density ($\rho_{\text{non-BC}}$) and spherical shape, as discussed in section 2.1. D_{d} (here $D_{\text{d}} = D_{\text{BC-shell}}$) and the dry coating amount (R_{D} and R_{m}) of the BC-containing particles are determined from m_{d} and the BC-core mass ($m_{\text{BC-core}}$) measured by SP2 incandescence signals, assuming the void-free density of the BC core ($\rho_{\text{BC-core}}$) and BC coating ($\rho_{\text{non-BC}}$) and core-shell geometry in equations (1) and (2). Note that in the APM-h-SP2 system, the dry BC-coating amount must be estimated by the APM method (*not* by the SP2-scattering method) in section 2.1. For ambient measurements, we assumed that $\rho_{\text{BC-core}} = 1.8\ \text{g cm}^{-3}$ and $\rho_{\text{non-BC}} = 1.5\ \text{g cm}^{-3}$, as discussed in section A2, where the assumptions made in the current measurement system were evaluated. The GF values of individual aerosol particles are determined from D_{d} and D for each particle:

$$\text{GF} = \frac{D}{D_{\text{d}}}. \tag{3}$$

The values of hygroscopicity parameter κ of individual particles are determined by the κ-Köhler theory [*Köhler*, 1936; *Petters and Kreidenweis*, 2007]:

$$\kappa = \left(\text{GF}^3 - 1\right)\left[\left\{\exp\left(\frac{4\sigma M_{\text{w}}}{RT\rho_{\text{w}} D_{\text{d}}\text{GF}}\right)\Big/\frac{\text{RH}(\%)}{100}\right\} - 1\right], \tag{4}$$

where ρ_{w} is the density of water, M_{w} is the molecular weight of water, σ is the surface tension at the solution-air interface, R is the universal gas constant, and T is the absolute temperature. The σ value is assumed to be equal to the surface tension of pure water. For clarity, the hygroscopicity parameter for BC-free particles is denoted as

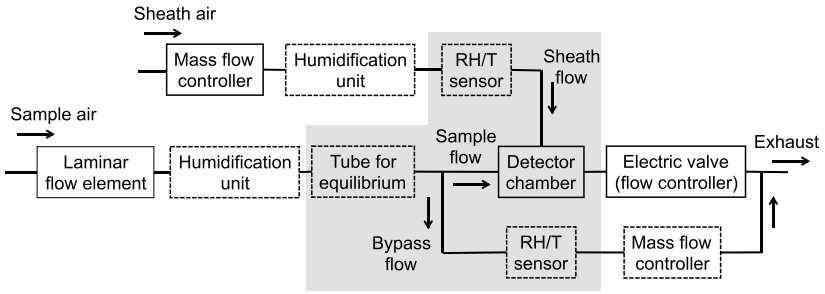

Figure 1. Flow system of the h-SP2. Components added to the original configuration of the standard SP2 are shown with dashed boxes. Thermally insulated components are shown with shaded boxes. Particle-free dry airflow to purge the optical detectors in the detector chamber (purge flow), which is employed in both the standard SP2 and the h-SP2, is not shown in the diagram for clarity.

$\kappa_{\text{BC-free}}$. For BC-containing particles, the hygroscopicity parameter of BC-coating materials ($\kappa_{\text{BC-coat}}$) can be derived from the overall κ by the mixing rule:

$$\kappa = \varepsilon_{\text{BC-core}}\kappa_{\text{BC-core}} + \varepsilon_{\text{BC-coat}}\kappa_{\text{BC-coat}}, \tag{5}$$

where $\kappa_{\text{BC-core}}$ is the hygroscopicity parameter of BC core, and $\varepsilon_{\text{BC-core}}$ and $\varepsilon_{\text{BC-coat}}$ are the volume fractions of BC core and BC-coating materials within the dry particle, respectively. Since bare BC particles show no detectable water uptake [e.g., *McMeeking et al*., 2011; *Schwarz et al*., 2015], the $\kappa_{\text{BC-core}}$ value is assumed to be 0. Then the equation (5) is reduced to

$$\kappa = \varepsilon_{\text{BC-coat}}\kappa_{\text{BC-coat}}. \tag{6}$$

Combining equations (4) and (6), $\kappa_{\text{BC-coat}}$ can be determined from the measured GF and $\varepsilon_{\text{BC-coat}}$.

To quantify the hygroscopic growth of BC-containing particles, the h-SP2 can be coupled with a standard (dry) SP2, instead of being coupled with the APM. *Schwarz et al*. [2015] developed a measurement system where a standard SP2 and an h-SP2 measure sample air in parallel. For BC-containing particles with a specific range of BC-core mass, water uptake is detected by comparing the optical sizing of this population between the humid and dry conditions. This system enables high time-resolved measurement of the average hygroscopic growth of BC-containing particles, which is suitable especially for aircraft observation. However, this system generally cannot measure the hygroscopic growth of BC-free particles and therefore does not provide simultaneous measurement data of $\kappa_{\text{BC-free}}$ and $\kappa_{\text{BC-coat}}$. Further, it is complicated by the need to relate measurements from different SP2s to each other at high precision.

2.3.2. Data-Processing Procedure

SP2 systems measure the differential scattering cross section integrated over the solid angle of SP2 detectors (ΔC_{sca}) by detecting scattered light from the individual particles. To derive optical diameter D of the particles from the measured ΔC_{sca} based on Mie theory, the refractive indices of the particles are required. However, due to particle water uptake in the h-SP2 system, the real part of the refractive indices of the original dry BC-free particles and BC-coating materials approach that of water (1.32) [e.g., *Schiebener et al*., 1990], affecting quantification of D from the measured ΔC_{sca}. For pure AS particles with the real part of the refractive index of 1.52, and with D_{d} of 200 nm, for instance, the volume-mixed refractive index of the particles decreases to 1.39 at GF = 1.5.

A data-processing algorithm is used to determine GF values for BC-free and BC-containing particles, taking into account the change in the refractive index due to particle water uptake. Figure 3 summarizes the data-processing procedure. For a BC-free particle, the diameter of the humidified particle is initially guessed. At the first iteration on the estimate of D, the value of D is set as $D_{\text{d}} + 1$ (nm). The refractive index of the humidified particle is then

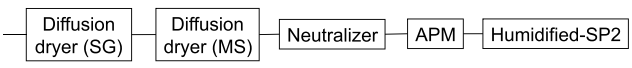

Figure 2. Schematic of the experimental setup for measurement of the hygroscopic growth of individual BC-free and BC-containing particles of a given mass (APM-h-SP2 method). SG, silica gel; MS, molecular sieves.

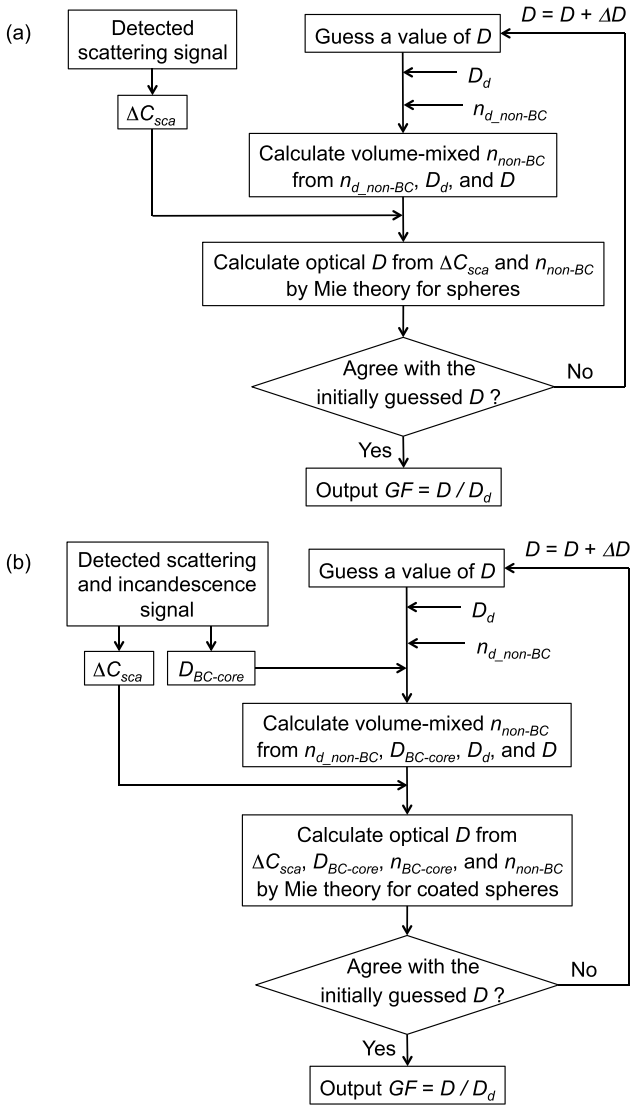

Figure 3. Data-processing procedure for the APM-h-SP2 method for (a) BC-free and (b) BC-containing particles. D, D_d, and $D_{BC\text{-}core}$ are the diameters of the humidified particle, dry particle, and BC core, respectively. D_d is determined from the dry particle mass selected by the APM, and the assumed densities of the non-BC and BC materials. $D_{BC\text{-}core}$ is determined from the incandescence signals detected by the h-SP2. ΔC_{sca} is the scattering cross section of the humidified particle measured by the h-SP2. $n_{d\_non\text{-}BC}$ and $n_{non\text{-}BC}$ are the refractive indices of the non-BC materials under the dry and humidified conditions, respectively. $n_{BC\text{-}core}$ is the refractive index of the BC core. GF is the growth factor calculated by D/D_d. Iteration on the estimate of D is carried out in 1 nm steps ($\Delta D = 1$ nm).

estimated from the volume mixing of the dry particle and water, assuming that particulate matter is uniformly dissolved in the humidified particles. For ambient BC-free particles with unknown composition, the refractive index of the dry particles is assumed to be that of AS. Using the estimated refractive index of the humidified particle, the diameter of the humidified particle is calculated by Mie theory from the ΔC_{sca} of the particle. The newly calculated diameter that agrees best with the initially guessed diameter should be the best estimate for the diameter of the humidified particle, and thus, the growth factor of the particle is determined. The criterion for the best agreement between the newly calculated and the initially guessed diameters is defined as the agreement to within ±20 nm. Iteration on the estimate of D is carried out in 1 nm steps. This data-processing algorithm for BC-free particles is a simplified version of that developed by *Sorooshian et al.* [2008] for the measurement of aerosol hygroscopicity using a differential mobility analyzer and RH-controlled optical particle counters. The data-processing procedure for a BC-containing particle is similar to that for a BC-free particle, except that a core-shell particle is assumed. Based on *Moteki et al.* [2010], the refractive indices of laboratory BC (fullerene soot (FS); Alpha Aeser, Inc., Wardhill, MA, USA, Stock Number 40971, Lot F12S011) and ambient BC particles are assumed to be $2.49 + 1.49i$ and $2.26 + 1.26i$, respectively. For measurement of ambient BC-containing particles, the refractive index of the dry coating materials is assumed to be that of AS.

If dry BC-free particles or BC-coating materials in the ambient air have a lower refractive index than that of AS, in the data-processing algorithm the measured ΔC_{sca} of the humidified particle is interpreted as a ΔC_{sca} of a smaller (less hygroscopic) particle with a higher refractive index, resulting in underestimates of the hygroscopic growth. The measurement uncertainty due to the assumptions in the algorithm including refractive indices is discussed in section A2.

2.3.3. Laboratory Experiments

The APM-h-SP2 measurement system was tested in the laboratory using both homogeneous AS and internally mixed particles of BC (FS) and AS. Homogeneous AS particles were produced by atomizing a pure AS

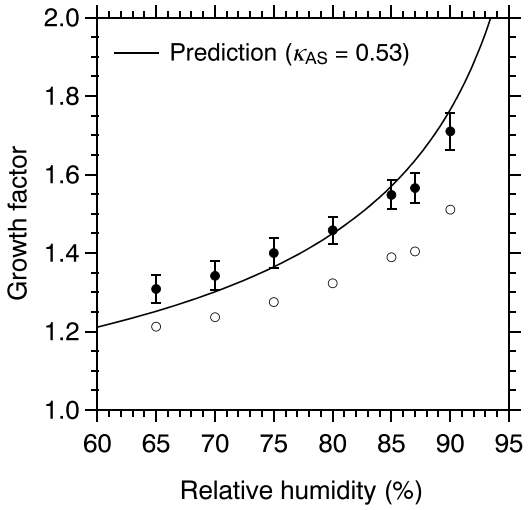

Figure 4. Measured (markers) and predicted (solid line) growth factors of AS as a function of RH. Closed circles show the measured growth factors using the data-processing algorithm described in section 2.3.2. Bars indicate the 25th–75th percentile. The measured median $\kappa_{BC\text{-}free}$ (here κ_{AS}) value at 85% RH was 0.50. Open circles show the measured growth factors for an assumed constant dry refractive index of AS.

solution, and internally mixed particles of FS and AS were generated by atomizing an AS solution containing FS. These particles were then dried with diffusion dryers, mass selected with the APM at 7.4 ± 1.2 fg ($D_d \sim 200$ nm), and then sampled over RH from 60% to 90%.

Figure 4 shows the measured hygroscopic growth of the pure AS particles. The histogram of the measured growth factor was bimodal. The fractions in the second mode (~10% to total) were multiply charged particles that passed through the APM and therefore were not included in the analysis. The measured growth factor generally agreed with the growth factor predicted by κ-Köhler theory ($\kappa_{AS} = 0.53$) [*Petters and Kreidenweis*, 2007], confirming the overall accuracy of the measurement system and the data-processing algorithm. The $\kappa_{BC\text{-}free}$ (here κ_{AS}) value measured at 85% RH was 0.50 (0.45–0.55 for 25–75 percentile), matching a priori knowledge of the κ_{AS} within uncertainties of ±6%. Note that this measurement uncertainty is valid for the well-characterized BC-free particles with known density and refractive index. As discussed in section A2, there are increased uncertainties for ambient BC-free particles with unknown composition. In Figure 4, for RH of the air in the detector chamber greater than 65%, all AS particles appeared to have deliquesced. This indicates that even though the average RH of the sample air in the SP2 detector chamber was controlled to be lower than the deliquescence RH of pure AS (79.9%), particles in the humidification unit likely experienced a higher RH than the deliquescence RH. During this experiment, to control RH of the sample air in the detection chamber, the temperature of the water bath in the humidification unit was controlled to be lower than the room temperature. Therefore, the temperature of the sample air in the humidification unit was also lower than that in the detection chamber (approximately room temperature), resulting in the higher RH at the exhaust of the humidification unit. Particles passing through near the wall of the Nafion tube may also experience higher RH because water vapor diffuses from there. The GF measured under the assumption of a constant refractive index was much smaller than that predicted, especially for higher RH conditions (Figure 4). This indicates that the reduction in the refractive index of the particles due to their water uptake must be taken into account for the estimates of GF.

Figure 5 shows the measured GF of the internally mixed particles of FS and AS. The thickly coated BC particles ($R_m = 6.4$–9.7; $R_D = 1.86$–2.14) showed larger GFs than those of the thinly coated BC particles ($R_m = 1.2$–1.8; $R_D = 1.07$–1.23). The measured GF for the thickly coated BC particles were consistent with those predicted by κ-Köhler theory. The $\kappa_{BC\text{-}coat}$ (here κ_{AS}) value measured at 85% RH was 0.48 (0.40–0.59 for 25–75 percentile), consistent with a priori knowledge of the κ_{AS} within uncertainties of ±10%. The larger dispersion of the data obtained for RH less than 70% is due to the fact that some particles deliquesced and others did not during the humidification process. For RH greater than 75%, all BC-containing particles appeared to have deliquesced. For BC particles with $R_m < 1.2$ ($R_D < 1.07$), no detectable hygroscopic growth was observed at any RH condition, confirming negligible water uptake by bare BC particles.

For the thinly coated BC particles ($R_m = 1.2$–1.8; $R_D = 1.07$–1.23), the measured GFs were substantially smaller than those predicted. This discrepancy is partly due to the assumption of a core-shell structure for the BC-containing particles. As discussed in section A1, where tests were conducted without humidification, the amount of coating on the thinly coated BC particles derived from the SP2-scattering and incandescence signals can be underestimated by about 50%. Here this results in an underestimate of the coating amount under humidified conditions, and a corresponding underestimate of the hygroscopicity of these particles. The accuracy of the estimate of the hygroscopic growth of thinly coated BC particles may be improved by estimating scattering cross sections of BC-containing particles assuming more realistic structures (that is, an aggregate of primary

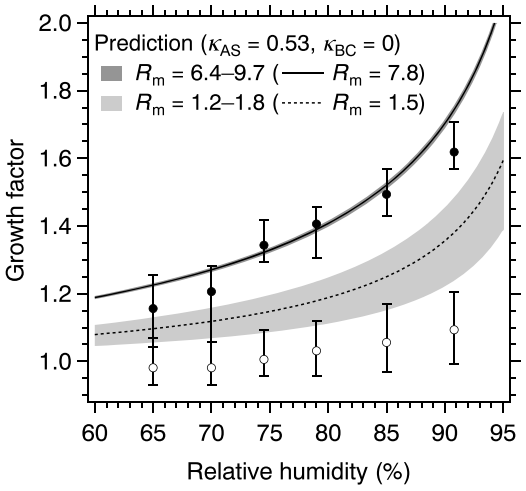

Figure 5. Measured and predicted growth factors of internally mixed particles of laboratory BC (FS) and AS as a function of RH. Measurement data for BC-containing particles with R_m (R_D) of 6.4–9.7 (1.86–2.14) and 1.2–1.8 (1.07–1.23) are shown by solid and open circles, respectively. The growth factors predicted for BC-containing particles are shown by dark and light shading, respectively. The predictions for R_m (R_D) of 7.8 (2.00) and 1.5 (1.15) are also shown by solid and dashed lines, respectively. Bars indicate the 25th–75th percentile. The measured median $\kappa_{BC\text{-}coat}$ (here κ_{AS}) values at 85% RH for these thickly and thinly coated BC particles are 0.48 and 0.11, respectively.

carbon spherules and non-BC compounds). In this study, however, the assumption of a core-shell model has been used exclusively.

Changes in particle morphology during humidification in the h-SP2 (and during aging process in the atmosphere for ambient BC particles) may also affect measurements of GFs. Previous studies have demonstrated that BC coatings of organic and inorganic acids and water can change BC-containing particles into less fractal, more compacted forms [e.g., *Pagels et al.*, 2009; *Miljevic et al.*, 2012]. In the APM-h-SP2 method, measurements of $m_{BC\text{-}core}$ (and thus $D_{BC\text{-}core}$) are not affected by the change in particle morphology because the incandescence signal is proportional to $m_{BC\text{-}core}$ for the particle with small size parameter [*Moteki and Kondo*, 2010]. However, the change in morphology can affect measurements of the humidified diameter D through the modification of scattering cross sections ΔC_{sca} of the particle. For both thinly and thickly coated BC particles, restructuring of BC-containing particle will make their morphologies closer to that assumed by the core-shell model. Nevertheless, for thinly coated BC particles (R_m = 1.2–1.8), the measured D (and thus GF) was substantially smaller than that predicted, possibly due to smaller degrees of restructuring for BC particles with thinner coatings.

Another possible cause for the underestimates of GF for thinly coated BC particles is due to the uncertainty of the classification of dry particles by the APM. In this study, dry particles with mass of 7.4 fg were selected by the APM. The mass resolution, that is, the width of the transfer function of the APM under our operational settings was theoretically estimated to be about ±1.2 fg [*Tajima et al.*, 2013]. In our data-processing procedure, the amount of dry BC coating for individual BC-containing particles is determined from the difference between APM-derived m_d (= 7.4 fg) and SP2-incandescence-derived $m_{BC\text{-}core}$. To analyze GF for thinly coated BC particles with R_m = 1.2–1.8 (R_D = 1.07–1.23), we chose particles with $m_{BC\text{-}core}$ of 4.0–6.1 fg ($D_{BC\text{-}core}$ = 162–186 nm) in the data analysis. Therefore, if these particles have m_d of about 6.2–7.4 fg (7.4–8.6 fg), then the hygroscopic growth of these particles should be less than (larger than) the predicted growth for particles with m_d = 7.4 fg, due to smaller (larger) amount of coating materials. In dry conditions, we found that 33% of BC particles with $m_{BC\text{-}core}$ of 4.0–6.1 fg were measured as bare BC particles ($R_D < 1.03$) by the SP2 scattering detection, and 20% of them were measured as larger coated particles ($R_D > 1.23$). Overall, this implies that a larger number of bare BC particles are counted as thinly coated BC particles, resulting in underestimates of hygroscopic growth of thinly coated BC particles in this experiment. Increasing the rotation frequency of the electrodes of the APM should improve the mass resolution and thus reduce measurement uncertainty due to the bare BC particles. However, this reduces the maximum height of the transfer function of the APM (i.e., more particles with a target m_d would be lost in the APM) and thus greatly reduced the number of particles detected by the h-SP2. For instance, if the rotation frequency is increased from the current setting of 5000 rotations per minute (RPM) to 10,000 RPM, the width of the transfer function of the APM would theoretically decrease from about ±1.2 fg to ±0.4 fg, while the maximum height of the transfer function decreases from 0.6 to 0.1.

The measurement uncertainty of the hygroscopic growth for thinly coated BC particles is larger than that for thickly coated BC particles, as analyzed above. The $\kappa_{BC\text{-}coat}$ (here κ_{AS}) value measured at 85% RH was 0.11 (0.0–0.34 for 25–75 percentile), showing 80% difference from a priori knowledge of the κ_{AS} (= 0.53). The difficulty in measuring $\kappa_{BC\text{-}coat}$ for thinly coated BC particles has been discussed also in *Schwarz et al.* [2015],

who compared scattering signals of BC-containing particles (with a specific BC-core mass) in dry and humidified conditions using SP2s.

3. Ambient Measurements

3.1. Observation Site

Our observation site was a temperature-controlled building in the Hongo campus of the University of Tokyo (35.71°N, 139.76°E), approximately 20 m above ground level. The observatory is located in the Tokyo Metropolitan Area (TMA) and is about 10 km northwest of the Tokyo Bay coastline. The site is in the highest carbon monoxide emission region within the TMA [*Kondo et al*., 2006, Figure 2]. Previous studies identified diesel emissions as a major source of BC in Tokyo [*Kondo et al*., 2006] and found that thinly coated BC particles ($R_D \sim 1.1$) were dominant in August and September in 2009 [*Kondo et al*., 2011].

We deployed the APM-h-SP2 measurement system during the field campaign Black Carbon/Carbonaceous Aerosol Removal Experiment in Tokyo (BC-CARE Tokyo) conducted for 20 days in July–August 2014. This campaign focused on the wet removal of BC-containing particles in Tokyo, which will be discussed in separate papers. In this paper, we present the measured hygroscopic growth of the BC-free and BC-containing particles with total dry mass of 7.4 fg ($D_d \sim 200$ nm) at 85% RH. The experimental setup of the APM-h-SP2 system was the same as that described in section 2.3. In this study, the dependence of the hygroscopicity on dry diameter (D_d) is not investigated, although chemical composition of nonrefractory aerosols may depend on dry particle size [e.g., *Zhang et al*., 2005]. Because the scattering signals of the h-SP2 are available only for the particles with optical diameter larger than about 170 nm, measurements of $\kappa_{BC\text{-}free}$ and $\kappa_{BC\text{-}coat}$ for smaller particles are difficult for the current APM-h-SP2 system. For larger particles, $\kappa_{BC\text{-}free}$ and $\kappa_{BC\text{-}coat}$ can be measured, but statistical significance is degraded due to greatly reduced number concentrations. Considering these constraints, dry particle mass selected by the APM was fixed at 7.4 fg ($D_d \sim 200$ nm) throughout the field campaign. Note that in this experimental setup, the measured coating thickness of BC decreases with the increase in the BC-core diameter. To interpret the hygroscopicity data, we also present the data of the chemical composition of nonrefractory (vaporized at 600°C under high vacuum) submicron aerosols measured by a quadrupole aerosol mass spectrometer (AMS) [*Jayne et al.,* 2000; *Takami et al.,* 2007], and the data of the total mass concentration of BC cores ($D_{BC\text{-}core} = 70$–850 nm) and the mixing states of BC particles measured by a standard SP2.

3.2. Results and Discussion

Figure 6 shows time series of the median GFs of BC-free and BC-containing particles during the observation period. The GFs of the BC-containing particles in Figure 6 were segregated by R_m (R_D). Thinly coated BC particles with $R_m = 1.2$–1.8 ($R_D = 1.08$–1.26) showed little or no detectable hygroscopic growth, whereas BC particles with coatings of $R_m = 4.2$–6.4 ($R_D = 1.69$–1.95) showed hygroscopic growth with GFs of ~1.2. The measured GFs of the thickly coated BC particles generally fell between those of thinly coated BC particles and those of BC-free particles. This is the first measurement of the temporal variations of the hygroscopic growth of particles in Tokyo, having been separated between BC-free and BC-containing particles.

The 1 h histograms of the measured GFs for the BC-free particles and those for the R_m-segregated BC-containing particles were generally bimodal during the observation period. The ratio of the number of the BC-free particles in the second mode to the total number of BC-free particles was 0.118. The ratios for BC-containing particles with $R_m = 1.8$–2.8, 2.8–4.2, 4.2–6.4, and 6.4–9.7 were 0.060, 0.089, 0.010, and 0.087, respectively. The particles in the second mode are considered to be multiply charged particles that had passed through the APM, and they were excluded from the present analysis, as detailed below. The ratio of BC-containing particles in the second mode with $R_m < 1.8$ could not be determined with accuracy. In order to exclude multiply charged particles, GF values greater than upper 10 percentile were first removed in determining the median GFs for the BC-free and the R_m-segregated BC-containing particles, although some of them could be singly charged particles with highly water activity. Because of our setting of m_d at 7.4 ± 1.2 fg, BC-containing particles with $m_{BC\text{-}core}$ larger than 9.2 fg were also regarded as multiply charged particles and removed in the data analysis.

Figure 7 shows the median GF distributions of BC-free and BC-containing particles during the observation period. In this figure, the GF distribution of the whole BC-containing particles is shown, without segregating

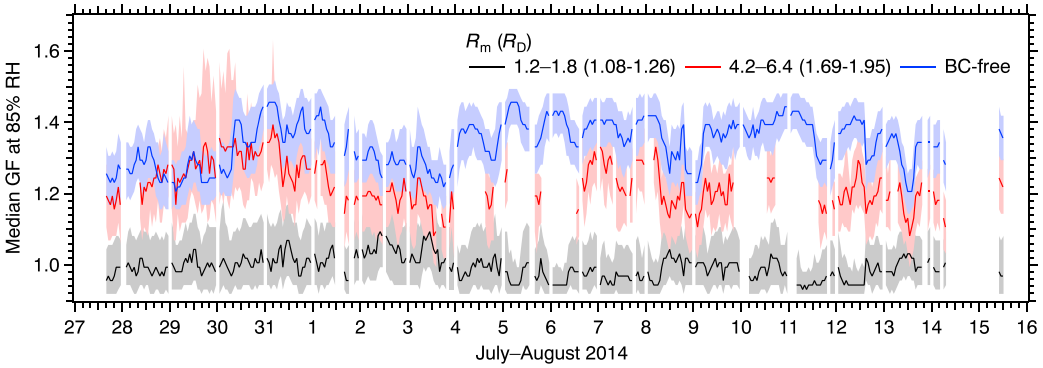

Figure 6. Time series (1 h data) of GFs at 85% RH for BC-free and BC-containing (R_m = 1.2–1.8 and 4.2–6.4) particles. m_d was set at 7.4 fg (D_d ~ 200 nm) by the APM. Solid lines show median GFs. Shading shows the range of the 25th–75th percentile. Data were not obtained during instrument maintenance. Statistically reliable data were not available when the number of particles detected in 1 h was less than 50.

the particles by R_m. The number fraction of BC-containing particles was about 10% of the whole (BC free + BC containing) particles of D_d ~ 200 nm. Particles with low GF (GF < 1.2) and with GF = 1.2–1.5 were dominant for BC-containing particles and BC-free particles, respectively. Particles with the measured GF of less than 1 resulted from the uncertainties of the assumed refractive indices, densities, and morphology of BC and non-BC materials. Throughout the observation period, the number fraction of the less-hygroscopic BC-containing particles (GF < 1.2; corresponding to critical supersaturation (S_c) > ~0.1%, based on κ-Köhler theory) was greater than 0.7. This dominance of thinly coated, less-hygroscopic BC particles in Tokyo air is characteristic of BC-containing particles in a megacity and consistent with the observation by *McMeeking et al.* [2011], who employed the HTDMA-SP2 system for observations in Manchester.

Figure 8a shows the time series of mass concentration of BC measured by the standard SP2 and that of each composition (organics and inorganics) measured by the AMS. The aerosol mass concentrations are given in the units of mass per unit volume of air at standard temperature and pressure (273.15 K and 1013.25 hPa). The average mass concentrations of BC, organics, SO_4^{2-}, NO_3^-, NH_4^+, and Cl^- during the observation period were 0.41, 6.6, 2.3, 0.61, 0.90, and 0.089 $\mu g\, m^{-3}$, respectively. Figure 8b shows the temporal variation of the median R_D of BC-containing particles with $D_{BC\text{-}core}$ = 186–214 nm measured by the standard SP2 with leading-edge scattering detection (SP2-scattering method (section 2.1)). In addition, the number fractions of BC-containing particles with $R_D > 1.2$ to the total number of the BC-containing particles ($D_{BC\text{-}core}$ 186–214 nm) are also shown in Figure 8b. The median R_D and the number fraction of $R_D > 1.2$ averaged over the observation period were 1.1 and 0.29, respectively.

Figure 8c shows the time variation of the distribution of the measured $\kappa_{BC\text{-}free}$. The median $\kappa_{BC\text{-}free}$ values of 0.2–0.4 fell between the κ value for pure ammonium sulfate (0.53) and those for some typical secondary organic aerosols (0.05–0.2) [e.g., *Huff Hartz et al.*, 2005; *VanReken et al.*, 2005; *Petters and Kreidenweis*, 2007; *King et al.*, 2009]. This result indicates that the majority of the BC-free particles was internally mixed with inorganic and organic aerosols, which is consistent with the observation by *Mochida et al.* [2006], who measured the hygroscopicity of aerosol particles by a HTDMA system in Tokyo. A few particles with $\kappa_{BC\text{-}free}$ of larger than ~ 0.6 in Figure 8c may be multiply charged particles. The APM-h-SP2 system measures $\kappa_{BC\text{-}free}$ on a single-particle basis and provides the $\kappa_{BC\text{-}free}$ distributions and thus provides information on the mixing states of the BC-free particles. This information is not obtained by bulk measurement of the aerosol chemical composition by the standard AMS method used in this study. In Figure 8d, the time series of the median $\kappa_{BC\text{-}free}$ measured by the h-SP2 is compared with that of the mass fraction of each composition measured by the AMS. The median $\kappa_{BC\text{-}free}$ reflected bulk compositional changes, confirming that the APM-h-SP2 system has an excellent sensitivity to the changes in chemical composition of the sampled aerosols.

Given the dry particle densities (ρ_{org}, ρ_{inorg}) and hygroscopicity parameters (κ_{org}, κ_{inorg}) of organics and inorganics, the values of $\kappa_{BC\text{-}free}$ can be estimated from the bulk chemical composition measured by the AMS, because the majority of the BC-free particles was likely internally mixed with organic and inorganic aerosols.

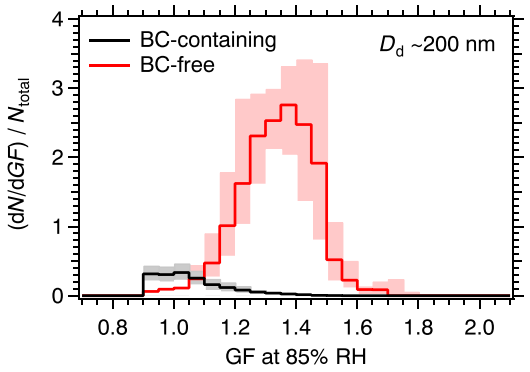

Figure 7. Medians of the normalized GF distributions (1 h data) of BC-free and BC-containing particles during the observation period. N_{total} is the total (BC free + BC containing) number concentration of the particles with D_d ~ 200 nm. Multiply charged particles were removed from the data set. Shading shows the range of the 25th–75th percentile.

Representing inorganic materials by ammonium sulfate ($\rho_{inorg} = 1.77\ g\ cm^{-3}$, $\kappa_{inorg} = 0.53$) and assuming $\rho_{org} = 1.2\ g\ cm^{-3}$ and $\kappa_{org} = 0.12$ for organic materials, the AMS-estimated $\kappa_{BC\text{-}free}$ agreed with the median $\kappa_{BC\text{-}free}$ measured by the h-SP2 to within ±20%, as shown in Figure 8e. It may also be said that if the values ρ_{inorg}, κ_{inorg}, and ρ_{org} are fixed, the assumed κ_{org} value of 0.05–0.2 explained the average of the h-SP2 median $\kappa_{BC\text{-}free}$ values during the observation period to within ±20%.

Figure 9a shows the diurnal variations of the median GFs of both BC-free and BC-containing particles. The median and 25–75 percentile values were calculated from the 1 h averaged GF data obtained during the 20 day period. The diurnal variations of aerosols in the TMA in summer are strongly influenced by transport processes, especially the development of the sea-land breeze circulation [*Kondo et al.*, 2008, 2010]. In the summer of 2014, large-scale air flow over Japan was strongly influenced by the North Pacific high, as usual. During the period between 4 and 8 August, the anticyclone covered the TMA and a stable sea-land breeze circulation developed. More detailed descriptions of the transport and its effect on photochemical processes in the TMA are given in *Kondo et al.* [2008, 2010]. Under the influence of this circulation, chemical aging of maritime air transported to the TMA proceeds after sunrise. BC concentrations were also observed to increase caused by increased emissions in the early morning [*Kondo et al.*, 2006].

The median GFs of BC-free particles were lowest at 1300–1800 local time (LT), generally corresponding to the high mass fractions of organics aerosols, as shown in Figure 9c. These results are consistent with *Takegawa et al.* [2006], who observed enhanced secondary organic aerosol (SOA) formation in the TMA during the daytime in summer. The diurnal variation of the GFs of BC-free particles was clearer during the period between 4 and 8 August. The GF values of BC-containing particles decreased in the early morning (0500–0900 LT), coinciding with the decrease in the number fractions of coated BC particles ($R_D > 1.2$; measured by the standard SP2 with SP2-scattering method (section 2.1)), as shown in Figure 9d. The corresponding observed increase in the BC mass concentration (Figure 9c) and decrease in the R_D in the morning, in turn, are interpreted to be due to the increased contributions of fresh BC from diesel vehicles in the TMA [*Kondo et al.*, 2006]. Thus, the measured GFs of BC-free and BC-containing particles generally showed different diurnal variations: relatively low GFs at daytime and at early morning for BC-free and BC-containing particles, respectively, and the relatively high GFs at night for both particles.

Figure 9b shows the diurnal variations of the median $\kappa_{BC\text{-}free}$ and the AMS-estimated $\kappa_{BC\text{-}free}$. They agreed with each other to within ±20%, except at 1800–2100 LT. At 1800–2100 LT, the median $\kappa_{BC\text{-}free}$ increased while the AMS-estimated $\kappa_{BC\text{-}free}$ decreased due to the increase in the organic mass fraction (Figure 9c). This difference suggests a formation of more hygroscopic (or higher density) organic aerosol during this period than assumed here ($\kappa_{org} = 0.12$, $\rho_{org} = 1.2\ g\ cm^{-3}$). *Takegawa et al.* [2006] introduced two possible mechanisms for the nighttime peaks in the mass concentrations of organic aerosols in Tokyo: a formation of SOA via reactions of volatile organic compounds (VOCs) with ozone and nitrogen oxides after sunset, and/or a shift in the gas/particle equilibrium of SOA compounds after sunset.

The measured $\kappa_{BC\text{-}free}$ values were compared with the measured $\kappa_{BC\text{-}coat}$ to investigate differences in their water activities. The $\kappa_{BC\text{-}coat}$ values were derived from thickly coated BC-containing particles with $R_m = 6.4$–9.7 ($R_D = 1.95$–2.25), because the uncertainty in the measured hygroscopic growth of thickly coated BC particles is relatively low (sections 2.3 and A2). Figure 8e shows the time variation of the median $\kappa_{BC\text{-}free}$ and median $\kappa_{BC\text{-}coat}$. The diurnal variation of the median $\kappa_{BC\text{-}coat}$ is not shown in Figure 9b, because the median $\kappa_{BC\text{-}coat}$ values were statistically unreliable during some periods, when the number of particles with $R_m = 6.4$–9.7 detected in 1 h was less than 50. Figure 10 shows a scatterplot of these values obtained during the observation period.

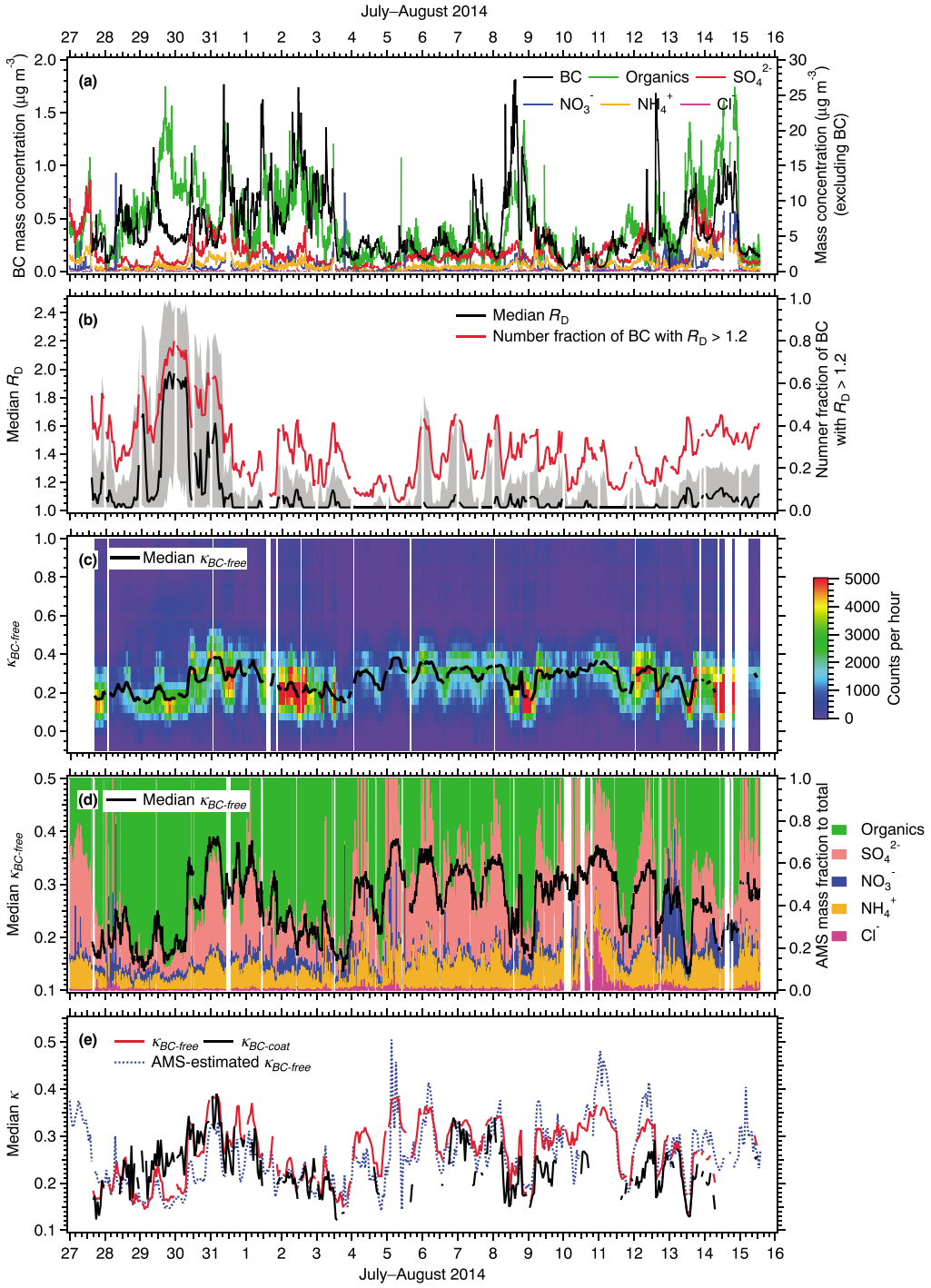

Figure 8. (a) Temporal variation (10 min data) of mass concentrations of BC, organics, SO_4^{2-}, NO_3^-, NH_4^+, and Cl^-. (b) Temporal variation (1 h data) of the median R_D of BC-containing particles with $D_{BC\text{-}core}$ = 186–214 nm. The lowest value of the measured R_D was set as 1.01 in the data analysis of the standard SP2. Shading shows the range of the 25th–75th percentile. The number fractions of the BC-containing particles with $R_D > 1.2$ to the total are also shown. (c) Temporal variation (1 h data) of the distribution of the hygroscopicity parameter $\kappa_{BC\text{-}free}$. The black line shows the median value. (d) Temporal variation (10 min data) of median $\kappa_{BC\text{-}free}$ and mass fractions of organics, SO_4^{2-}, NO_3^-, NH_4^+, and Cl^- versus the total mass of aerosols with diameters of less than about 1 μm. (e) Temporal variation (1 h data) of median $\kappa_{BC\text{-}free}$ and median $\kappa_{BC\text{-}coat}$. The $\kappa_{BC\text{-}coat}$ values were derived from the thickly coated BC particles with R_m = 6.4–9.7 (R_D = 1.95–2.25). One hour average data are not shown when the number of particles detected in 1 h was less than 50. The $\kappa_{BC\text{-}free}$ estimated from the bulk chemical composition is also shown.

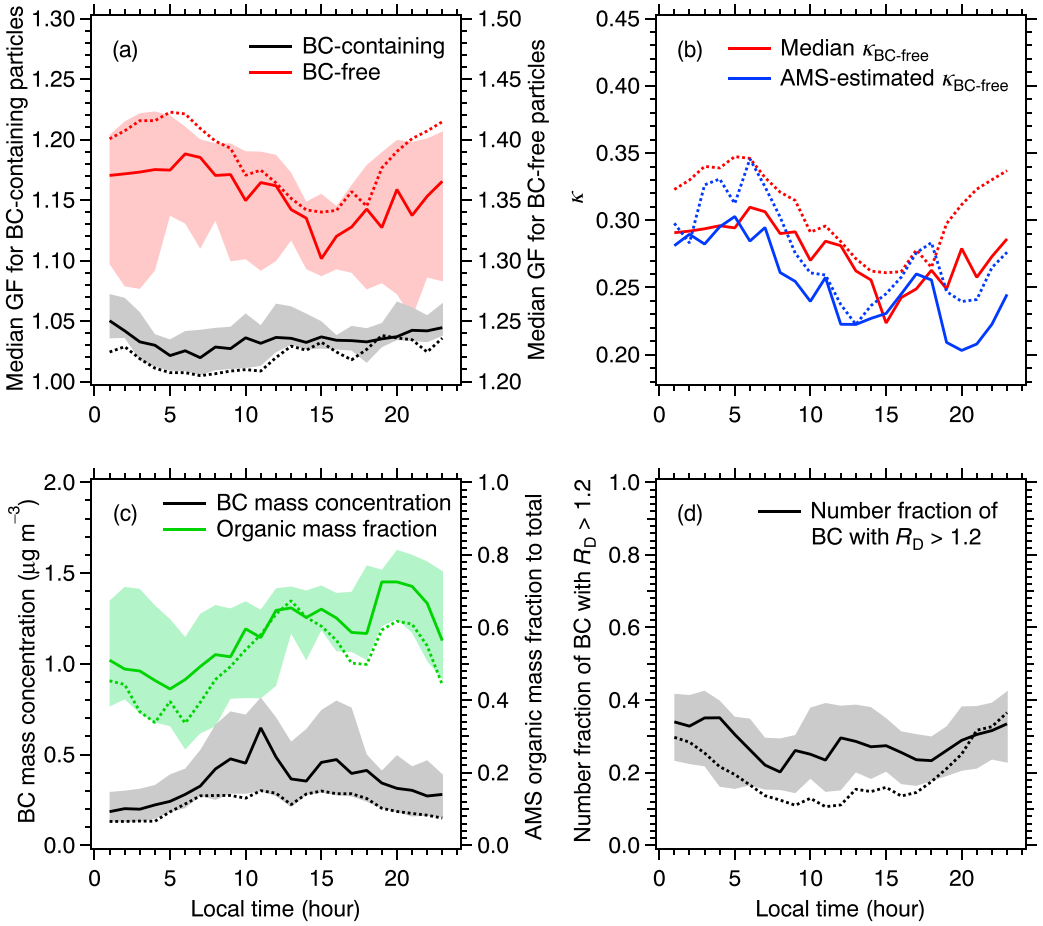

Figure 9. Diurnal variations (1 h data) of (a) the median GFs of BC-free and BC-coating particles ($D_d \sim 200$ nm) at 85% RH, (b) the median $\kappa_{BC\text{-}free}$ and $\kappa_{BC\text{-}free}$ estimated from the bulk chemical composition, (c) the BC mass concentration ($D_{BC\text{-}core} = 70–850$ nm) and mass fractions of organics versus the total mass of aerosols with diameters of less than about 1 μm, and (d) number fractions of BC-containing particles with $R_D > 1.2$ to the total number of the BC-containing particles ($D_{BC\text{-}core} = 186–214$ nm). The solid line shows the median data during the observation period. Shading shows the range of the 25th–75th percentile. The dashed lines show the median data during the period between 4 and 8 August, when the Tokyo Metropolitan Area was covered by the North Pacific high and a stable sea-land breeze circulation prevailed.

The median $\kappa_{BC\text{-}free}$ and $\kappa_{BC\text{-}coat}$ values were well correlated ($R^2 = 0.68$), except for the period during 29–30 July 2014, and agreed to within ±25% during most of the observation period (~81%). Figure 11 shows correlation plots of the median $\kappa_{BC\text{-}free}$ and $\kappa_{BC\text{-}coat}$ against mass fractions of organics and SO_4^{2-} measured by the AMS. The AMS-estimated $\kappa_{BC\text{-}free}$ is also shown in Figure 11a as a function of the organic mass fraction. The median $\kappa_{BC\text{-}free}$ and $\kappa_{BC\text{-}coat}$ values correlated negatively with the AMS organic and positively with SO_4^{2-} mass fractions, although the R^2 values for the $\kappa_{BC\text{-}coat}$ were much lower than those for $\kappa_{BC\text{-}free}$. The median $\kappa_{BC\text{-}free}$ and $\kappa_{BC\text{-}coat}$ also correlated positively with NH_4^+ mass fractions with $R^2 = 0.49$ and $R^2 = 0.11$, respectively, while they did not correlate with NO^{3-} and Cl^- mass fractions (not shown). The similarity between the median $\kappa_{BC\text{-}free}$ and $\kappa_{BC\text{-}coat}$ values (Figure 10) and the correlations between these values and AMS data (Figure 11) suggest that the BC-free particles and BC-coating materials generally had similar chemical compositions (i.e., internal mixture of inorganic and organic compounds) and hence were formed in the atmosphere via similar physicochemical processes.

The similarity between $\kappa_{BC\text{-}free}$ and $\kappa_{BC\text{-}coat}$ observed in this study was limited to thickly coated BC particles ($R_m = 6.4–9.7$; $R_D = 1.95–2.25$). These BC particles constituted only about 6.5% on average of the whole BC-containing particles with $m_d = 7.4$ fg ($D_d \sim 200$ nm) during the observation period. Another method of direct quantification of chemical compositions of BC-free and BC-containing particles is the use of a soot particle aerosol mass spectrometer (SP-AMS) [*Onasch et al.*, 2012]. *Lee et al.* [2015] recently utilized an SP-AMS

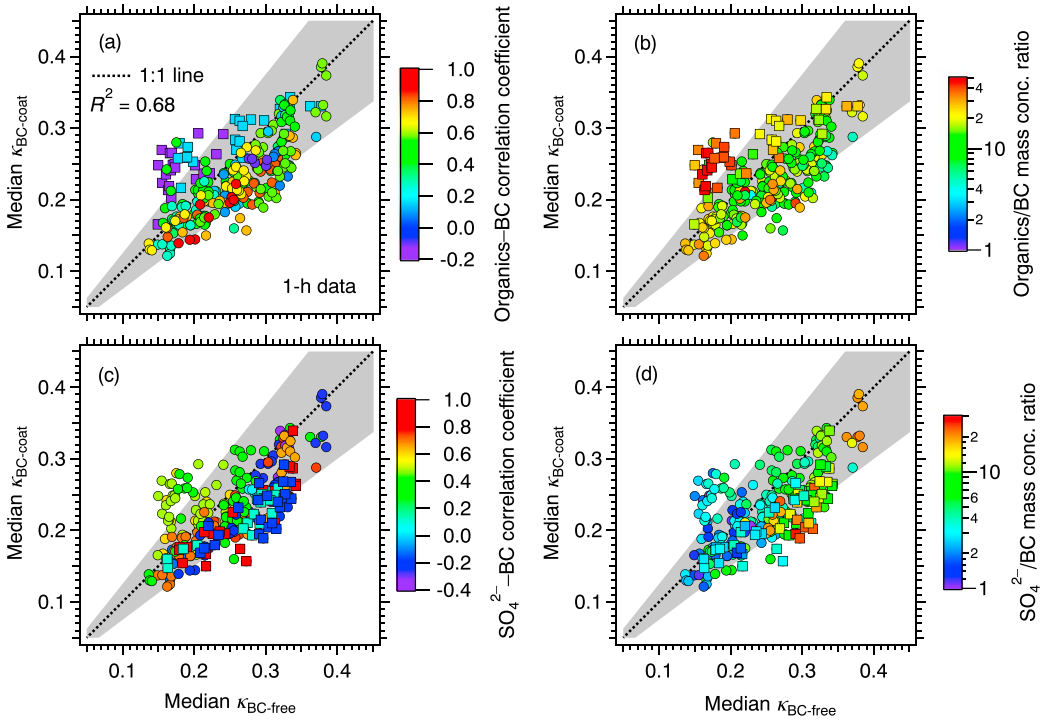

Figure 10. Scatterplot of the median $\kappa_{BC\text{-}free}$ and $\kappa_{BC\text{-}coat}$ (1 h data) during the observation period. The $\kappa_{BC\text{-}coat}$ values were derived from the thickly coated BC particles with R_m = 6.4–9.7 (R_D = 1.95–2.25). Shading shows the range of ±25%. (a) Squares show the data obtained during 29–30 July 2014, and circles show the rest of the data. Colors show the daily correlation coefficient between mass concentrations of BC and organic aerosols. (b) As in Figure 10a, but colors show the 1 h data of the organic aerosols/BC mass concentration ratio. (c) Squares show the data obtained during 8–9 and 12 August 2014, and circles show the rest of the data. Colors show the daily correlation coefficient between mass concentrations of BC and sulfate ion. (d) As in Figure 10c, but colors show the 1 h data of the sulfate ion/BC mass concentration ratio.

equipped with a light scattering module and measured aerosol chemical composition in an urban environment both on a single-particle basis and on an ensemble (bulk) basis.

The APM-h-SP2 system has been shown to provide information on the composition and mixing states of BC-containing and BC-free particles, in terms of their hygroscopicity. These results indicate that on average, the chemical composition of BC-coating materials is represented by that of BC-free aerosols measured by an AMS as a first approximation. Thus, the hygroscopicity of BC-containing particles can be estimated by approximating $\kappa_{BC\text{-}coat}$ as $\kappa_{BC\text{-}free}$ in equation (6), if the volume fractions of BC-coating materials within the particle ($\varepsilon_{BC\text{-}coat}$) are properly taken into account. This is a common assumption, and the present observations prove its general validity. This will hold if the precursors of non-BC materials (e.g., VOCs and sulfur dioxide (SO_2)) are coemitted with BC within time scales of their aging to enable simultaneous condensation of their oxidation products onto BC and BC-free particles, although primary coatings upon emissions from diesel vehicles or biomass burning may contribute to the difference between $\kappa_{BC\text{-}free}$ and $\kappa_{BC\text{-}coat}$. Collisions of BC-containing and BC-free particles should not alter the similarity between $\kappa_{BC\text{-}free}$ and $\kappa_{BC\text{-}coat}$.

However, this similarity was not universally observed during the field campaign. The median $\kappa_{BC\text{-}coat}$ was much higher than that of $\kappa_{BC\text{-}free}$ during the period of 29–30 July, when the correlation between the mass concentrations of BC and organic aerosols was lowest. Figure 10a shows color-coded daily correlation coefficient (R) between the total mass concentrations of BC and organic aerosols, which were derived from 10 min data of the standard SP2 and AMS. It is likely that during this poor-correlation period, the sources of BC and organic aerosols were quite different, and the coating materials of BC had relatively high inorganic/organic ratios compared to that of BC-free particles. In fact, during this period the mass concentrations of BC were better correlated with those of sulfate ($R \sim 0.5$) than those of organics ($R \sim \pm 0.2$), as shown in Figure 10c. In addition, the highest organic aerosol/BC mass concentration ratio was observed during this period as well (Figure 10b), also supporting the difference in the origins between BC and organic aerosols. The opposite behavior was observed during the

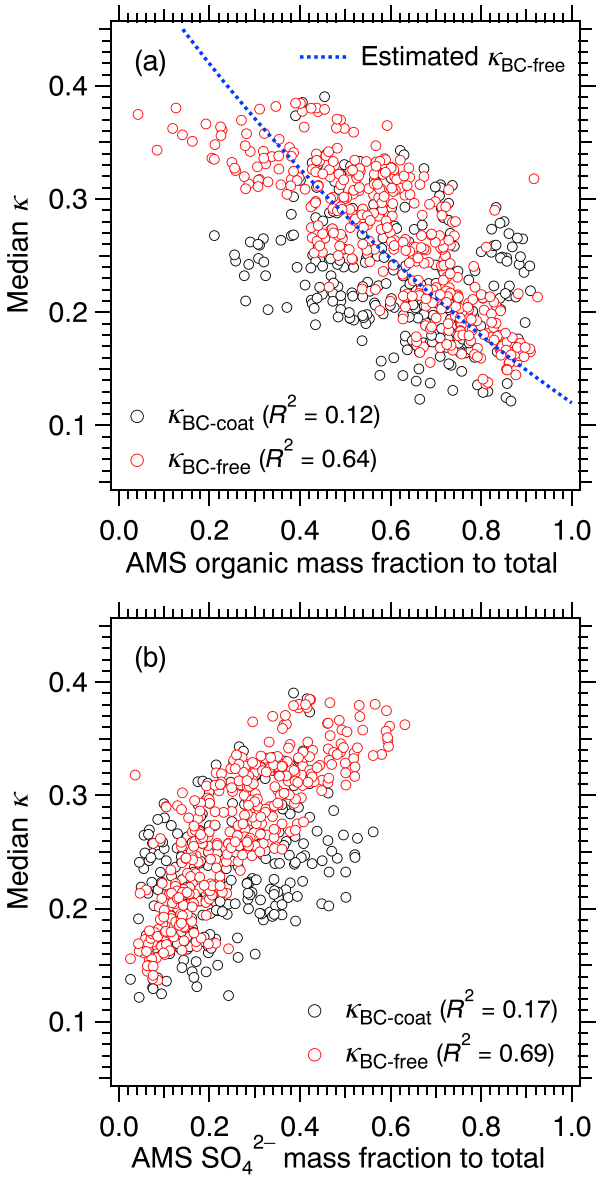

Figure 11. Scatterplots of the median $\kappa_{BC\text{-}free}$ and $\kappa_{BC\text{-}coat}$ (1 h data) against mass fractions of (a) organics and (b) SO_4^{2-} to the total mass of aerosols with diameters of less than about 1 μm. In Figure 11a, the $\kappa_{BC\text{-}free}$ estimated from the organic mass fractions is also shown (dashed lines).

period of 8–9 and 12 August, when the correlation between the mass concentrations of BC and sulfate was relatively low (Figure 10c). It is likely that during this period, the inorganic fractions of the coating materials of BC were considerably lower than those of BC-free particles. Accordingly, lower $\kappa_{BC\text{-}coat}$ values were also observed when the sulfate/BC mass concentration ratio reached ~30 (Figure 10d).

These results indicate that BC-coating materials and BC-free particles were, on this occasion, formed by different processes at different stages during transport of air parcels before reaching the observation site. Because simultaneous measurements of $\kappa_{BC\text{-}coat}$ and $\kappa_{BC\text{-}free}$ have not been broadly explored, further measurements under different environmental conditions are needed to further elucidate their behaviors. Such measurements will contribute to improved understanding of the sources (anthropogenic and natural) of organic or inorganic aerosols externally mixed with BC, if the types of the BC sources are known, and may also be relevant to improved understanding of secondary aerosol production.

The observed difference between $\kappa_{BC\text{-}coat}$ and $\kappa_{BC\text{-}free}$ also indicates that estimating CCN activity of BC-containing particles from the AMS-derived, bulk $\kappa_{BC\text{-}free}$ values should be associated with increased uncertainties. The median $\kappa_{BC\text{-}coat}$ measured on 30 July, for instance, was ~0.26, whereas the AMS-estimated $\kappa_{BC\text{-}free}$ was ~0.16. For a BC-containing particle with $D_{BC\text{-}core}$ = 100 nm and R_D = 1.1 (a typical value of R_D in Tokyo), the estimated critical supersaturations (S_c) were 0.39% and 0.49% for coating κ of 0.26 and 0.16, respectively, based on κ-Köhler theory. The difference between the estimated S_c can thus be significant, which motivates further measurements of $\kappa_{BC\text{-}coat}$ and $\kappa_{BC\text{-}free}$ under a wider range of environmental conditions to improve understanding of CCN activity and removal of BC-containing particles in the atmosphere.

Measurements of $\kappa_{BC\text{-}coat}$ as a function of R_m (R_D) are not presented in this study because of the relatively large uncertainty in the measurement of the hygroscopic growth for thinly coated BC particles. BC particles can be thinly coated by organic aerosols upon emissions from diesel vehicles [*Toner et al.*, 2006; *Shields et al.*, 2007]. However, in this study it is difficult to estimate water activity ($\kappa_{BC\text{-}coat}$) of the thin coatings with the current APM-h-SP2 system.

4. Summary and Conclusion

We measured the hygroscopicity parameter κ of BC-coating materials ($\kappa_{BC\text{-}coat}$) and BC-free particles ($\kappa_{BC\text{-}free}$) in the urban atmosphere of Tokyo using a humidified SP2 (h-SP2) sampling mass-selected aerosol.

In the measurement system, an APM selected dry aerosol particles with specific mass, and then, at controlled RH, the h-SP2 quantified the BC mass content and optical diameter of each aerosol particle by detecting laser-induced incandescence and the scattered light. Laboratory tests with homogeneous ammonium sulfate (AS) particles and BC particles internally mixed with AS showed that the measured growth factors (GFs) of the pure AS and thickly coated BC particles were consistent with those predicted by κ-Köhler theory. The $\kappa_{\text{BC-free}}$ and $\kappa_{\text{BC-coat}}$ values were derived from the measured GFs at 85% RH, and matched a priori knowledge of the κ of AS within uncertainties of ±10% and ±80% for thickly and thinly coated BC particles and ±6% for BC-free particles. For ambient particles with unknown compositions, the measurement uncertainties of κ for thickly coated BC particles and BC-free particles were estimated to be ±45% and ±42%, respectively, by changing the assumed densities. It was difficult to measure the κ of thin coatings for ambient BC-containing particles with the current measurement system.

Throughout the observation period, the number fraction of BC-containing particles with low hygroscopicity (GF $<$ 1.2 at 85% RH, or critical supersaturation (S_c) $>$ ~0.1%) was greater than 70% of the total BC-containing particles with a dry diameter of about 200 nm. The measured $\kappa_{\text{BC-free}}$ and $\kappa_{\text{BC-coat}}$ were mostly between the hygroscopicities of typical inorganic and organic aerosols, suggesting that individual BC-free particles and BC-coating materials were internally mixed with inorganic and organic compounds.

The measured median $\kappa_{\text{BC-free}}$ and $\kappa_{\text{BC-coat}}$ values were well correlated ($R^2 = 0.68$) and agreed to within ±25%, indicating that the chemical compositions of BC-free particles and BC-coating materials were similar on average. This holds if the precursors of non-BC materials (e.g., VOCs and SO_2) are coemitted with BC within time scales of their aging, followed by condensation of their oxidation products onto BC and BC-free particles.

We also found that the difference between the $\kappa_{\text{BC-free}}$ and $\kappa_{\text{BC-coat}}$ was occasionally significant, when the mass concentrations of BC and the other aerosols were poorly correlated, and/or the mass concentration of the other aerosols is considerably higher than that of BC. This indicates the formation of BC-coating materials and BC-free particles by different processes and at different stages during the transport of air parcels before reaching the observation site. These measurements will be useful for investigating the types of sources of aerosols.

The measured $\kappa_{\text{BC-coat}}$ values are useful for the studies of CCN activation and wet removal of BC-containing particles observed during the field campaign, which will be discussed in separate papers.

Appendix A

A1. Measurements of the Dry BC-Coating Amounts Using an SP2

To evaluate the validity of the SP2 measurements of the BC-coating amount, the dry shell/core diameter ratio (R_D) of the laboratory BC particles was measured using the experimental setup shown in Figure A1. Ammonium sulfate (AS) was added to a water suspension of fullerene soot (FS) and then atomized to generate internally mixed BC particles. The total dry mass of the individual BC-containing particles (m_d) was set to be 7.4 ± 1.2 fg by the APM. Masses of the BC cores ($m_{\text{BC-core}}$) are measured from each incandescence signal; therefore, in addition to the measurements of R_D via SP2 leading-edge scattering signals (SP2-scattering method), the amount of coating materials (here AS) is determined from the difference between the m_d and the $m_{\text{BC-core}}$ for each particle (APM method), as described in section 2.1.

In Figure A2, the R_D measured by the APM method is compared with the R_D measured by the SP2-scattering method, where assumptions of core-shell structure, refractive indices of BC and AS, and void-free densities of BC and AS are made. The coating thicknesses (= ($D_{\text{BC-shell}} - D_{\text{BC-core}}$)/2) for BC-containing particles with a relatively thick coating (R_D greater than about 1.3) agreed to within 12%. However, for thinly coated BC particles with R_D of about 1.19, the coating thickness via the SP2-scattering method was smaller by 44% than that via the APM method. This shows larger relative uncertainty for thin coatings by the SP2 scattering

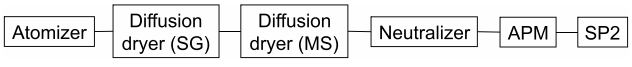

Figure A1. Schematic of the experimental setup for the laboratory measurement of the dry shell/core ratio of BC-containing particles of a given mass. SG, silica gel; MS, molecular sieves.

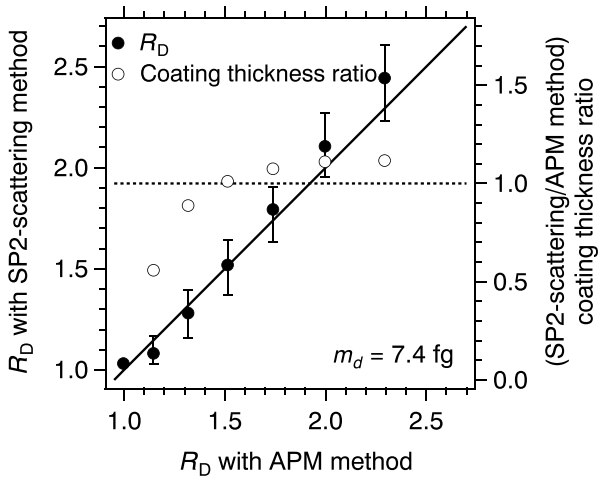

Figure A2. Dry shell/core diameter ratios (R_D) of laboratory BC particles (FS) internally mixed with AS measured via the dry particle mass selected by the APM (APM method) versus those measured via the leading edge of the SP2-scattering signals (SP2-scattering method) are shown by solid circles. Bars indicate the 25th–75th percentile. The solid line shows the 1:1 line. For both methods, masses of the BC cores were derived from the incandescence signals of the SP2. For data analysis of the SP2-scattering method, we assumed a core-shell structure, a refractive index of FS of $2.49 + 1.49i$ at $\lambda = 1064$ nm [*Moteki et al.,* 2010], and a refractive index of AS of $1.52 + 0i$, a void-free density of BC of 1.8 g cm^{-3}, and a void-free density of AS of 1.77 g cm^{-3}. For particles with a R_D of 1 (i.e., bare FS), the measured R_D should not have any bias for both methods, since the refractive index of bare FS particles was measured assuming the density of BC of 1.8 g cm^{-3} and spherical particles by *Moteki et al.* [2010]. The (SP2-scattering/APM method) coating thickness ratios were shown by open circles, except for particles with R_D of ~1. The dashed line shows the coating thickness ratio of 1.

detection and is qualitatively consistent with underestimates of hygroscopic growth for thinly coated BC particles in laboratory experiments (section 2.3.3). For thinly coated BC particles, scattering cross sections can be more affected by their nonspherical shape.

For the analysis of the laboratory experiments using fullerene soot described in this section and in section 2.3.3, we assumed the values of $\rho_{BC\text{-}core} = 1.8$ g cm^{-3} and $n_{BC\text{-}core} = 2.49 + 1.49i$, based on *Moteki et al.* [2010]. *Moteki et al.* [2010] determined the $n_{BC\text{-}core}$ values of fullerene soot and the other BC samples assuming this $\rho_{BC\text{-}core}$ and a spherical shape of BC particles. Figure 6 of *Schwarz et al.* [2015] also showed a good agreement between the measured scattering cross sections ΔC_{sca} of fullerene soot and those predicted by Mie theory under the assumptions of $\rho_{BC\text{-}core} = 1.8$ g cm^{-3} and $n_{BC\text{-}core} = 2.49 + 1.49i$. In other words, there was a good agreement between $D_{BC\text{-}core}$ derived from the measured $m_{BC\text{-}core}$ assuming $\rho_{BC\text{-}core} = 1.8$ g cm^{-3} and $D_{BC\text{-}core}$ derived from the measured ΔC_{sca} assuming $n_{BC\text{-}core} = 2.49 + 1.49i$. Therefore, estimating R_D by the SP2 scattering method assuming these $\rho_{BC\text{-}core}$ and $n_{BC\text{-}core}$ values based on the core-shell model should be reasonable, although the uncertainties of the $\rho_{BC\text{-}core}$ and $n_{BC\text{-}core}$ values are not quantified. In the APM method, on the other hand, R_D is derived from the measured m_d and $m_{BC\text{-}core}$ assuming only the value of $\rho_{BC\text{-}core}$. The assumed $\rho_{BC\text{-}core}$ of 1.8 g cm^{-3} is well within the reported range of $\rho_{BC\text{-}core}$ for graphitic and non-graphitic carbons [*Moteki et al.,* 2010, and references therein]. The consistency between the R_D measured by the SP2-scattering method and the R_D measured by the APM method in Figure A2 also supports the validity of the assumed $\rho_{BC\text{-}core}$ for fullerene soot. For ambient BC particles in Tokyo, *Moteki et al.* [2010] reported $n_{BC\text{-}core} = 2.26 + 1.26i$ under the assumption of $\rho_{BC\text{-}core} = 1.8$ g cm^{-3}. These values were used for the analysis of the field observation described in section 3.

A2. Uncertainty of the Hygroscopicity Measurement

Several assumptions are made in determining the growth factors for ambient (unknown) BC-free and BC-containing particles by the APM-h-SP2 method. The dry particle densities $\rho_{BC\text{-}core}$ and $\rho_{non\text{-}BC}$ are assumed in order to derive D_d from the APM-selected m_d. In addition, the dry refractive indices $n_{BC\text{-}core}$ and $n_{d\_non\text{-}BC}$ at $\lambda = 1064$ nm are assumed in the data-processing procedure (section 2.3.2). It is also assumed that non-BC materials are completely dissolved in the humidified particles. Determination of D for BC-free and BC-containing particles is based on Mie theory assuming spherical shapes.

Table A1. The Hygroscopicity of Ambient BC-Free and BC-Containing Particles (D_d ~ 200 nm) Measured by the APM-h-SP2 Method Under Various Assumptions[a]

			Measured Median Values	
Particle Type	Assumption Type	Assumed Values	GF at 85% RH	$\kappa_{BC\text{-}free}$ or $\kappa_{BC\text{-}coat}$
BC-free particles	Standard	$\rho_{non\text{-}BC} = 1.5$ g cm^{-3}, $n_{d\_non\text{-}BC} = 1.52 + 0i$	1.34	0.26
	High density	$\rho_{non\text{-}BC} = 1.8$ g cm^{-3}	1.44	0.37
	Low density	$\rho_{non\text{-}BC} = 1.2$ g cm^{-3}	1.22	0.15
	Low refractive index	$n_{d\_non\text{-}BC} = 1.45 + 0i$	1.38	0.30
BC-containing particles (R_m = 6.4–9.7; R_D = 1.95–2.25)	Standard	$\rho_{BC\text{-}core} = 1.8$ g cm^{-3}, $\rho_{non\text{-}BC} = 1.5$ g cm^{-3}, $n_{BC\text{-}core} = 2.26 + 1.26i$, $n_{d\_non\text{-}BC} = 1.52 + 0i$	1.27	0.22
	High density	$\rho_{non\text{-}BC} = 1.8$ g cm^{-3}	1.35	0.32
	Low density	$\rho_{non\text{-}BC} = 1.2$ g cm^{-3}	1.17	0.12
	Low core refractive index	$n_{BC\text{-}core} = 2 + 1i$	1.29	0.24
	Low coating refractive index	$n_{d\_non\text{-}BC} = 1.45 + 0i$	1.30	0.26
BC-containing particles (R_m = 1.8–2.8; R_D = 1.26–1.46)	Standard	$\rho_{BC\text{-}core} = 1.8$ g cm^{-3}, $\rho_{non\text{-}BC} = 1.5$ g cm^{-3}, $n_{BC\text{-}core} = 2.26 + 1.26i$, $n_{d\_non\text{-}BC} = 1.52 + 0i$	1.06	NA
	High density	$\rho_{non\text{-}BC} = 1.8$ g cm^{-3}	1.10	NA
	Low density	$\rho_{non\text{-}BC} = 1.2$ g cm^{-3}	1.02	NA
	Low core refractive index	$n_{BC\text{-}core} = 2 + 1i$	1.13	NA
	Low coating refractive index	$n_{d\_non\text{-}BC} = 1.45 + 0i$	1.08	NA

[a]Time series of median GF and κ (1 h data) measured on 8 August 2014 in Tokyo were averaged. NA: not available.

The uncertainties due to the assumed densities and refractive indices are estimated by changing their values within their possible ranges and reanalyzing the raw data obtained by the APM-h-SP2 system. This study is summarized in Table A1. The particle densities of AS aerosol and ammonium nitrate aerosol, which are typical inorganic aerosols in the atmosphere, are 1.77 and 1.72 g cm^{-3}, respectively. Although atmospheric organic aerosols include numerous kinds of species, literature values suggest that 1.2 g cm^{-3} is a reasonable estimate for the organic aerosol density [*Turpin and Lim*, 2001, and references therein]. *McMurry et al.* [2002] measured the densities of urban aerosol particles of size ~100 and ~300 nm to be 1.54–1.77 g cm^{-3}, depending on the abundance of organic and inorganic aerosols during the observation period. Considering these previous studies, $\rho_{non\text{-}BC} = 1.5$ g cm^{-3} was used as a reference value in analyzing the ambient data obtained by the APM-h-SP2 system with a range of 1.2–1.8 g cm^{-3}. A value of $\rho_{BC\text{-}core} = 1.8$ g cm^{-3} was used for BC cores, as described in section A1.

The real part of the refractive index of AS near infrared is 1.50–1.53 [*Toon et al.*, 1976]. According to *Hess et al.* [1998], the real part of the refractive index of water-soluble and water-insoluble aerosols (excluding BC and dust) at $\lambda = 1000$ nm is 1.52. On the basis of the reported values of refractive indices at various wavelengths [e.g., *Stelson*, 1990; *Ebert et al.*, 2002], the real part of the refractive index of BC-free particles is likely within the range 1.43–1.58. Taking these reported values into consideration, $n_{d\_nonBC} = 1.52 + 0i$ was used in analyzing ambient APM-h-SP2 data. A value of $n_{BC\text{-}core} = 2.26 + 1.26i$ was used for BC core, as described in section A1. Because this $n_{BC\text{-}core}$ value was determined assuming $\rho_{BC\text{-}core} = 1.8$ g cm^{-3} [*Moteki et al.*, 2010], these $n_{BC\text{-}core}$ and $\rho_{BC\text{-}core}$ values are related with each other. Here we examine the sensitivity of the measured GF to the assumed value of $n_{BC\text{-}core}$, not to that of $\rho_{BC\text{-}core}$.

Table A1 shows the hygroscopicity of ambient BC-free and BC-containing particles measured by the APM-h-SP2 method under the various assumptions. Data were collected on 8 August 2014 in Tokyo during a field campaign (section 3). For BC-free particles, the sensitivities of the derived hygroscopic growth to the assumed density and refractive index were tested by changing the density by ±20% from the reference value or by setting a low refractive index of $1.45 + 0i$. The measured GF and $\kappa_{BC\text{-}free}$ were 1.34 ± 0.12 and 0.26 ± 0.11 (±42%), respectively, corresponding to the changes in $\rho_{non\text{-}BC}$. The effects of the assumed $n_{d\_BC\text{-}free}$ on measurements were relatively small. For BC-containing particles, the uncertainty associated with the refractive index of the BC core ($n_{BC\text{-}core} = 2 + 1i$) were also evaluated, in addition to the effects of changing the assumed density and refractive index of the BC coating on GF measurements. For BC-containing particles with $R_m = 6.4$–9.7 ($R_D = 1.95$–2.25), the measured GF and $\kappa_{BC\text{-}coat}$ were 1.27 ± 0.10 and 0.22 ± 0.10 (±45%), respectively, when changing the $\rho_{non\text{-}BC}$ by ±20%. The effects of the assumed density were greater than those of the assumed refractive indices of the BC core

and BC coating. For BC-containing particles with $R_m = 1.8–2.8$ ($R_D = 1.26–1.46$), the measured GF was more sensitive to the value of $n_{BC\text{-}core}$ (or $\rho_{BC\text{-}core}$) than to the $\rho_{non\text{-}BC}$ and $n_{d\_non\text{-}BC}$ values.

The assumption of the shape of the BC-containing particles (that is, the core–shell model) and the resolution of particle-mass selection by the APM also cause uncertainty, as discussed in sections 2.3 and A1. For thinly coated BC particles with $R_m = 1.2–1.8$ ($R_D = 1.07–1.23$), the measurement uncertainty of $\kappa_{BC\text{-}coat}$ even for well-characterized BC-containing particles was estimated to be ±80% by laboratory experiments in section 2.3. The $\kappa_{BC\text{-}coat}$ values for ambient BC-containing particles with thin coatings were thus highly uncertain and not shown in Table A1.

Acknowledgments

This work was supported by the Ministry of Education, Culture, Sports, Science, and Technology (MEXT), the global environment research fund of the Japanese Ministry of the Environment (A-1101 and 2-1403), the Japan Society for the Promotion of Science (JSPS) KAKENHI grants 12J06736 and 23221001, and the GRENE Arctic Climate Change Research Project, and the Arctic Challenge for Sustainability (ArCS) project. The authors thank T. Miyoshi and H. Nara for operating an AMS during the field campaign in Tokyo and M. Irwin for laboratory support. The data used in this study will be available upon request to the authors (ohata@eps.s.u-tokyo.ac.jp).

References

Bond, T. C., et al. (2013), Bounding the role of black carbon in the climate system: A scientific assessment, *J. Geophys. Res. Atmos.*, *118*, 5380–5552, doi:10.1002/jgrd.50171.

Chuang, P. Y. (2003), Measurement of timescale of hygroscopic growth for atmospheric aerosols, *J. Geophys. Res.*, *108*(D9), 4282, doi:10.1029/2002JD002757.

Duplissy, J., et al. (2009), Intercomparison study of six HTDMAs: Results and recommendations, *Atmos. Meas. Tech.*, *2*, 363–378, doi:10.5194/amt-2-363-2009.

Ebert, M., S. Weinbruch, A. Rausch, G. Gorzawski, P. Hoffmann, H. Wex, and G. Helas (2002), Complex refractive index of aerosols during LACE 98 as derived from the analysis of individual particles, *J. Geophys. Res.*, *107*(D21), 8121, doi:10.1029/2000JD000195.

Gao, R. S., et al. (2007), A novel method for estimating light–scattering properties of soot aerosols using a modified single–particle soot photometer, *Aerosol Sci. Technol.*, *41*, 125–135.

Hess, M., P. Koepke, and I. Schult (1998), Optical properties of aerosols and clouds: The software package OPAC, *Bull. Am. Meteorol. Soc.*, *79*, 831–844.

Huff Hartz, K. E., T. Rosenørn, S. R. Ferchak, T. M. Raymond, M. Bilde, N. M. Donahue, and S. N. Pandis (2005), Cloud condensation nuclei activation of monoterpene and sesquiterpene secondary organic aerosol, *J. Geophys. Res.*, *110*, D14208, doi:10.1029/2004JD005754.

Intergovernmental Panel on Climate Change (2013), *IPCC Fifth Assessment Report: Climate Change 2013*, Cambridge Univ. Press, Cambridge, U. K.

Jayne, J. T., D. C. Leard, X. Zhang, P. Davidovits, K. A. Smith, C. E. Kolb, and D. R. Worsnop (2000), Development of an aerosol mass spectrometer for size and composition analysis of submicron particles, *Aerosol Sci. Technol.*, *33*, 49–70.

King, S. M., T. Rosenoern, J. E. Shilling, Q. Chen, and S. T. Martin (2009), Increased cloud activation potential of secondary organic aerosol for atmospheric mass loadings, *Atmos. Chem. Phys.*, *9*, 2959–2971.

Köhler, H. (1936), The nucleus in and the growth of hygroscopic droplets, *Trans. Faraday Soc.*, *32*, 1152–1161.

Kondo, Y. (2015), Effects of black carbon on climate: Advances in measurement and modeling, *Monogr. Environ. Earth Planets*, *3*, 1–85, doi:10.5047/meep.2015.00301.0001.

Kondo, Y., et al. (2006), Temporal variations of elemental carbon in Tokyo, *J. Geophys. Res.*, *111*, D12205, doi:10.1029/2005JD006257.

Kondo, Y., et al. (2008), Formation and transport oxidized reactive nitrogen, ozone, and secondary organic aerosol in Tokyo, *J. Geophys. Res.*, *113*, D21310, doi:10.1029/2007JD010134.

Kondo, Y., et al. (2010), Formation and transport of aerosols in Tokyo in relation to their physical and chemical properties—A review, *J. Meteorol. Soc. Jpn.*, *88*, 597–624.

Kondo, Y., L. Sahu, N. Moteki, F. Khan, N. Takegawa, X. Liu, M. Koike, and T. Miyakawa (2011), Consistency and traceability of black carbon measurements made by laser-induced incandescence, thermal-optical transmittance, and filter-based photo-absorption techniques, *Aerosol Sci. Technol.*, *45*, 295–312.

Laborde, M., P. Mertes, P. Zieger, J. Dommen, U. Baltensperger, and M. Gysel (2012), Sensitivity of the single particle soot photometer to different black carbon types, *Atmos. Meas. Tech.*, *5*, 1031–1043.

Lee, A. K. Y., M. D. Willis, R. M. Healy, T. B. Onasch, and J. P. D. Abbatt (2015), Mixing state of carbonaceous aerosol in an urban environment: Single particle characterization using the soot particle aerosol mass spectrometer (SP-AMS), *Atmos. Chem. Phys.*, *15*, 1823–1841, doi:10.5194/acp-15-1823-2015.

Liu, D., J. Allan, J. Whitehead, D. Young, M. Flynn, H. Coe, G. McFiggans, Z. L. Fleming, and B. Bandy (2013), Ambient black carbon particle hygroscopic properties controlled by mixing state and composition, *Atmos. Chem. Phys.*, *13*, 2015–2029, doi:10.5194/acp-13-2015-2013.

Matsui, H., M. Koike, Y. Kondo, N. Moteki, J. D. Fast, and R. A. Zaveri (2013), Development and validation of a black carbon mixing state resolved three-dimensional model: Aging processes and radiative impact, *J. Geophys. Res. Atmos.*, *118*, 2304–2326, doi:10.1029/2012JD018446.

McMeeking, G. R., N. Good, M. D. Petters, G. McFiggans, and H. Coe (2011), Influences on the fraction of hydrophobic and hydrophilic black carbon in the atmosphere, *Atmos. Chem. Phys.*, *11*, 5099–5112, doi:10.5194/acp-11-5099-2011.

McMurry, P. H., X. Wang, K. Park, and K. Ehara (2002), The relationship between mass and mobility for atmospheric particles: A new technique for measuring particle density, *Aerosol Sci. Technol.*, *36*, 227–238.

Miljevic, B., N. C. Surawski, T. Bostrom, and Z. D. Ristovski (2012), Restructuring of carbonaceous particles upon exposure to organic and water vapours, *J. Aerosol Sci.*, *47*, 48–57.

Mochida, M., M. Kuwata, T. Miyakawa, N. Takegawa, K. Kawamura, and Y. Kondo (2006), Relationship between hygroscopicity and cloud condensation nuclei activity for urban aerosols in Tokyo, *J. Geophys. Res.*, *111*, D23204, doi:10.1029/2005JD006980.

Moteki, N., and Y. Kondo (2007), Effects of mixing state of black carbon measurement by laser-induced incandescence, *Aerosol Sci. Technol.*, *41*, 398–417.

Moteki, N., and Y. Kondo (2010), Dependence of laser-induced incandescence on physical properties of black carbon aerosols: Measurements and theoretical interpretation, *Aerosol Sci. Technol.*, *44*, 663–675.

Moteki, N., Y. Kondo, Y. Miyazaki, N. Takegawa, Y. Komazaki, G. Kurata, T. Shirai, D. R. Blake, T. Miyakawa, and M. Koike (2007), Evolution of mixing state of black carbon particles: Aircraft measurements over the western Pacific in March 2004, *Geophys. Res. Lett.*, *34*, L11803, doi:10.1029/2006GL02894334.

Moteki, N., Y. Kondo, and S. Nakamura (2010), Method to measure refractive indices of small nonspherical particles: Application to black carbon particles, *J. Aerosol Sci.*, *41*, 513–521.

Onasch, T. B., A. Trimborn, E. C. Fortner, J. T. Jayne, G. L. Kok, L. R. Williams, P. Davidovits, and D. R. Worsnop (2012), Soot particle aerosol mass spectrometer: Development, validation, and initial application, *Aerosol Sci. Technol.*, *46*(7), 804–817.

Oshima, N., M. Koike, Y. Zhang, and Y. Kondo (2009), Aging of black carbon in outflow from anthropogenic sources using a mixing state resolved model: 2. Aerosol optical properties and cloud condensation nuclei activities, *J. Geophys. Res.*, *114*, D18202, doi:10.1029/2008JD011681.

Pagels, J., A. F. Khalizov, P. H. McMurry, and R. Y. Zhang (2009), Processing of soot by controlled sulphuric acid and water condensation–mass and mobility relationship, *Aerosol Sci. Technol.*, *43*, 629–640.

Petters, M. D., and S. M. Kreidenweis (2007), A single parameter representation of hygroscopic growth and cloud condensation nucleus activity, *Atmos. Chem. Phys.*, *7*, 1961–1971.

Petzold, A., et al. (2013), Recommendations for reporting "black carbon" measurements, *Atmos. Chem. Phys.*, *13*, 8365–8379.

Schiebener, P., J. Straub, J. M. H. Levelt Sengers, and J. S. Gallagher (1990), Refractive index of water and steam as function of wavelength, temperature, and density, *J. Phys. Chem. Ref. Data*, *19*, 677–717, doi:10.1063/1.555859.

Schneider, J., N. Hock, S. Weimer, S. Borrmann, U. Kirchner, R. Vogt, and V. Scheer (2005), Nucleation particles in diesel exhaust: Composition inferred from in situ mass spectrometric analysis, *Environ. Sci. Technol.*, *39*(16), 6153–6161.

Schwarz, J. P., et al. (2006), Single-particle measurement of mid latitude black carbon and light-scattering aerosols from the boundary layer to the lower stratosphere, *J. Geophys. Res.*, *111*, D16207, doi:10.1029/2006JD007076.

Schwarz, J. P., A. E. Perring, M. Z. Markovic, R. S. Gao, S. Ohata, J. Langridge, D. Law, R. McLaughlin, and D. W. Fahey (2015), Technique and theoretical approach for quantifying the hygroscopicity of black-carbon-containing aerosol using a single particle soot photometer, *J. Aerosol Sci.*, *81*, 110–126.

Shields, L. G., D. T. Suess, and K. A. Prather (2007), Determination of single particle mass spectral signatures from heavy-duty diesel vehicle emissions for PM 2.5 source apportionment, *Atmos. Environ.*, *41*(18), 3841–3852.

Shiraiwa, M., Y. Kondo, N. Moteki, N. Takegawa, Y. Miyazaki, and D. R. Blake (2007), Evolution of mixing state of black carbon in polluted air from Tokyo, *Geophys. Res. Lett.*, *34*, L16803, doi:10.1029/2007GL029819.

Shiraiwa, M., Y. Kondo, N. Moteki, N. Takegawa, L. K. Sahu, A. Takami, S. Hatakeyama, S. Yonemura, and D. R. Blake (2008), Radiative impact of mixing state of black carbon aerosol in Asian outflow, *J. Geophys. Res.*, *113*, D24210, doi:10.1029/2008JD010546.

Sjogren, S., M. Gysel, E. Weingartner, U. Baltensperger, M. J. Cubison, H. Coe, A. A. Zardini, C. Marcolli, U. R. Krieger, and T. Peter (2007), Hygroscopic growth and water uptake kinetics of two-phase aerosol particles consisting of ammonium sulphate, adipic and humic acid mixtures, *J. Aerosol Sci.*, *38*, 157–171.

Sorooshian, A., S. Hersey, F. J. Brechtel, A. Corless, R. C. Flagan, and J. H. Seinfeld (2008), Rapid, size-resolved aerosol hygroscopic growth measurements: Differential aerosol sizing and hygroscopicity spectrometer probe (DASH-SP), *Aerosol Sci. Technol.*, *42*, 445–464.

Stelson, A. W. (1990), Urban aerosol refractive index prediction by molar refraction approach, *Environ. Sci. Technol.*, *24*, 1676–1679.

Stephens, M., N. Turner, and J. Sandberg (2003), Particle identification by laser-induced incandescence in a solid-state laser cavity, *Appl. Opt.*, *42*, 3726–3736.

Tajima, N., H. Sakurai, N. Fukushima, and K. Ehara (2013), Design considerations and performance evaluation of a compact aerosol particle mass analyzer, *Aerosol Sci. Technol.*, *47*, 1152–1162.

Takami, A., T. Miyoshi, A. Shimono, N. Kaneyasu, S. Kato, Y. Kajii, and S. Hatakeyama (2007), Transport of anthropogenic aerosols from Asia and subsequent chemical transformation, *J. Geophys. Res.*, *112*, D22S31, doi:10.1029/2006JD008120.

Takegawa, N., T. Miyakawa, Y. Kondo, J. L. Jimenez, Q. Zhang, D. R. Worsnop, and M. Fukuda (2006), Seasonal and diurnal variations of submicron organic aerosol in Tokyo observed using the Aerodyne aerosol mass spectrometer, *J. Geophys. Res.*, *111*, D11206, doi:10.1029/2005JD006515.

Toner, S. M., D. A. Sodeman, and K. A. Prather (2006), Single particle characterization of ultrafine and accumulation mode particles from heavy duty diesel vehicles using aerosol time-of-flight mass spectrometry, *Environ. Sci. Technol.*, *40*(12), 3912–3921.

Toon, O. B., J. B. Pollack, and B. N. Khare (1976), The optical constants of several atmospheric aerosol species: Ammonium sulfate, aluminum oxide, and sodium chloride, *J. Geophys. Res.*, *81*, 5733–5748.

Turpin, B. J., and H. Lim (2001), Species contributions to PM2.5 mass concentrations: Revisiting common assumptions for estimating organic mass, *Aerosol Sci. Technol.*, *35*, 602–610.

VanReken, T. M., N. L. Ng, R. C. Flagan, and J. H. Seinfeld (2005), Cloud condensation nucleus activation properties of biogenic secondary organic aerosol, *J. Geophys. Res.*, *110*, D07206, doi:10.1029/2004JD005465.

Zhang, Q., M. R. Canagaratna, J. T. Jayne, D. R. Worsnop, and J. L. Jimenez (2005), Time and size resolved chemical composition of submicron particles in Pittsburgh: Implications for aerosol sources and processes, *J. Geophys. Res.*, *110*, D07S09, doi:10.1029/2004JD004649.

Zhang, R. Y., A. F. Khalizov, J. Pagels, D. Zhang, H. Xue, and P. H. McMurry (2008), Variability in morphology, hygroscopicity, and optical properties of soot aerosols during atmospheric processing, *Proc. Natl. Acad. Sci. U.S.A.*, *105*, 10,291–10,296, doi:10.1073/pnas.0804860105.